Institut de recherche
Robert-Sauvé en santé
et en sécurité du travail

An Assessment of Methods of Sampling and Characterizing Engineered Nanomaterials in the Air and on Surfaces in the Workplace

Maximilien Debia
Gilles L'Espérance
Cyril Catto
Philippe Plamondon
André Dufresne
Claude Ostiguy

STUDIES AND RESEARCH PROJECTS

R-1009

CHEMICAL AND BIOLOGICAL
HAZARD PREVENTION RESEARCH

OUR RESEARCH
is working for you !

The Institut de recherche Robert-Sauvé en santé et en sécurité du travail (IRSST), established in Québec since 1980, is a scientific research organization well-known for the quality of its work and the expertise of its personnel.

Mission

To contribute, through research, to the prevention of industrial accidents and occupational diseases and to the rehabilitation of affected workers;

To disseminate knowledge and serve as a scientific reference centre and expert;

To provide the laboratory services and expertise required to support the public occupational health and safety network.

Funded by the Commission des normes, de l'équité, de la santé et de la sécurité du travail, the IRSST has a board of directors made up of an equal number of employer and worker representatives.

To find out more

Visit our Web site for complete up-to-date information about the IRSST. All our publications can be downloaded at no charge.
www.irsst.qc.ca

To obtain the latest information on the research carried out or funded by the IRSST, subscribe to our publications:

- *Prévention au travail,* the free magazine published jointly by the IRSST and the CNESST (preventionautravail.com)
- InfoIRSST, the Institute's electronic newsletter

Legal Deposit
Bibliothèque et Archives nationales du Québec
2018
ISBN : 978-2-89797-016-1
ISSN : 0820-8395

IRSST – Communications and Knowledge
Transfer Division
505 De Maisonneuve Blvd. West
Montréal, Québec
H3A 3C2
Phone: 514 288-1551
publications@irsst.qc.ca
www.irsst.qc.ca

An Assessment of Methods of Sampling and Characterizing Engineered Nanomaterials in the Air and on Surfaces in the Workplace

Maximilien Debia[1], Gilles L'Espérance[2], Cyril Catto[1], Philippe Plamondon[2], André Dufresne[1] et Claude Ostiguy[1,3]

[1]Département de santé environnementale et santé au travail, École de santé publique, Université de Montréal
[2]Centre de caractérisation microscopique des matériaux, Polytechnique Montréal
[3]IRSST

STUDIES AND RESEARCH PROJECTS

R-1009

This study was funded by the IRSST. The conclusions and recommendations are solely those of the authors.
This publication is a translation of the French original; only the original version (R-952) is authoritative.

PEER REVIEW
In compliance with IRSST policy, the research results
published in this document have been peer-reviewed.

ACKNOWLEDGEMENTS

The authors would like to thank the following for their contributions to this project: Charlotte Allard, Michèle Bouchard, Denis Dieme, Etienne Dubé, Claude Émond, France Gagnon, Serge Kouassi, Jens Kroeger, Olivier Christian Mudaheranwa, Igor Pujalte, Brigitte Roberge and Michaela Skulinova.

We would also like to thank all those in the workplaces studied who made it possible for us to carry out the studies.

Lastly, we would like to thank the Institut de recherche Robert-Sauvé en santé et en sécurité du travail (IRSST) and Prima Québec (formerly NanoQuébec) for funding the project.

ABSTRACT

The monitoring of air contamination by engineered nanomaterials (ENM) is a complex process with many uncertainties and limitations owing to the presence of particles of nanometric size that are not ENMs, the lack of validated instruments for breathing zone measurements and the many indicators to be considered. In addition, some organizations, France's Institut national de recherche et de sécurité (INRS) and Québec's Institut de recherche Robert-Sauvé en santé et en sécurité du travail (IRSST) among them, stress the need to also sample surfaces for ENM deposits. In other words, existing methods of sampling and characterizing ENMs need to be fine-tuned and new ones developed to get a better picture of the risks of occupational exposure. Accordingly, the main goal of this project was to develop innovative methodological approaches for detailed qualitative as well as quantitative characterization of occupational exposure to ENMs.

This research project has two complementary parts: a laboratory investigation and a fieldwork component. The laboratory investigation (Part A) involved generating titanium dioxide (TiO_2) nanoparticles under controlled laboratory conditions and studying different sampling and analysis devices. The fieldwork (Part B) comprised a series of nine field studies customized to each specific workplace and designed to test a variety of sampling devices and analytical procedures and to measure ENM exposure levels among Québec workers.

The methods for characterizing aerosols and surface deposits that were investigated include: i) measurement by direct-reading instruments (DRI), such as condensation particle counters (CPC), optical particle counters (OPC), laser photometers, aerodynamic diameter spectrometers and electric mobility spectrometers; ii) transmission electron microscopy (TEM) or scanning electron microscopy (SEM) using a variety of sampling devices, including the Mini Particle Sampler® (MPS); iii) measurement of elemental carbon (EC); iv) inductively coupled plasma mass spectrometry (ICP-MS) and (v) Raman spectroscopy.

The fieldwork covered a variety of industries (e.g., electronics, manufacturing, printing, construction, energy, research and development) and included producers as well as users or integrators of ENMs. In the workplaces studied, we found nanometals or metal oxides (TiO_2, SiO_2, zinc oxides, lithium iron phosphate, titanate, copper oxides), nanoclays, nanocellulose and carbonaceous materials, including carbon nanofibres (CNFs) and carbon nanotubes (CNTs)—single-walled (SWCNTs) as well as multiwalled (MWCNTs).

The project helped to advance our knowledge of occupational exposure to ENMs by documenting specific tasks and industrial processes (e.g., printing and varnishing), as well as certain less investigated ENMs (nanocellulose, for example).

Based on our investigations, we propose a strategy for more accurate assessment of ENM exposure using methods that require a minimum of preanalytical handling. The recommended strategy is a systematic two-step assessment of workplaces that produce and use ENMs. The first step involves testing with different DRIs (such as a CPC and a laser photometer) as well as sample collection and subsequent microscopy analysis (MPS + SEM/TEM) to clearly identify work tasks that generate ENMs. The second step, once occupational exposure is confirmed, is

specific quantification of the ENMs detected. The following results are particularly helpful for detailed characterization of ENM exposure:

i. The first conclusive tests of a technique using ICP-MS to quantify the metal oxide content of samples collected in the workplace

ii. The possibility of combining different sampling methods recommended by the National Institute for Occupational Safety and Health (NIOSH) to measure EC as an NTC/NFC indicator, as well as demonstration of the limitation of this method stemming from observed interference with the black carbon particles required to synthesize carbon materials (for example, Raman spectroscopy showed that less than 6% of the particles deposited on the microscopy grids at one site were SWCNTs)

iii. The clear advantages of using the MPS® (instead of standard 37-mm cassettes) for sampling onto an electron microscopy grid, allowing quantification of the materials collected

iv. The major impact of sampling time: a long sampling time overloads microscopy grids and can lead to overestimation of average particle agglomerate size and underestimation of particle concentrations

v. The feasibility and utility of surface sampling, either with sampling pumps or by passive diffusion onto microscopy grids, to assess ENM dispersion in the workplace

These original results suggest promising avenues for assessing ENM exposure, while also showing some of their limitations. Improvements to our sampling and analysis methods give us a better understanding of ENM exposure and help in adapting and implementing control measures that can minimize occupational exposure.

TABLE OF CONTENTS

LIST OF TABLES

LIST OF FIGURES

ABBREVIATIONS

AIHA	American Industrial Hygiene Association
APS	Aerodynamic particle sizer
BN	Background noise
CNT	Carbon nanotube
CNF	Carbon nanofiber
CPC	Condensation particle counter
DRI	Direct-reading instrument
EC	Elemental carbon
EDS	Energy-dispersive x-ray spectroscopy
EEPS	Engine exhaust particle sizer
ELPI	Electrical low-pressure impactor
EM	Electron microscopy
ENM	Engineered nanomaterial
ESPUM	*École de santé publique de l'Université de Montréal* (school of public health, University of Montreal)
FMPS	Fast mobility particle sizer
ICP-MS	Inductively coupled plasma mass spectrometry
INÉRIS	*Institut national de l'environnement industriel et des risques* (France's national institute of industrial safety and environmental protection)
INRS	*Institut national de recherche et de sécurité* (France's national research and safety institute)
IRSST	*Institut de recherche Robert-Sauvé en santé et en sécurité du travail* (Québec occupational health and safety research institute)
MCE	Mixed cellulose ester
MPS	Mini Particle Sampler®
MRV	Minimum reporting value
MWCNT	Multiwalled carbon nanotube
NIOSH	National Institute for Occupational Safety and Health (NIOSH)
NP	Nanoparticle
NT	Nanotechnology
OPC	Optical particle counter
PPI	Parallel particle impactor
PTFE	Polytetrafluoroethylene
SEM	Scanning electron microscopy
SMPS	Scanning mobility particle sizer
SWCNT	Single-walled carbon nanotube
STEM	Scanning transmission electron microscopy
TEM	Transmission electron microscopy
UFP	Ultrafine particle

1. RESEARCH QUESTION

1.1 Background and introduction

The work described here is the logical follow-up to the investigations undertaken by our team with the support of the *Institut de recherche Robert-Sauvé en santé et en sécurité du travail* (IRSST) regarding the assessment of exposure to nanoparticles (NPs), including ultrafine particles (UFPs) and engineered nanomaterials (ENMs).

A first project[1] funded by the IRSST enabled a preliminary characterization of NP exposure among aluminum smelter workers and apprentice welders using condensation particle counters (CPCs). This exploratory work, the first to document NP exposure in Québec, recommended further investigations to characterize exposure, in particular by broadening and diversifying exposure indicators to be assessed (Debia et al., 2012a).

Next, a best practices guide was improved and updated,[2] bringing together "current scientific knowledge on hazard identification, strategies for determining nanomaterial levels in different work environments, risk assessment and the application of various risk management approaches." The update made it possible to conduct a series of investigations in different work environments, which in turn highlighted the need for a case-by-case approach. It also showed that there is still no consensus on a measurement method for characterizing occupational exposure to nanomaterials, making quantitative risk assessment difficult if not impossible in many situations (Ostiguy et al., 2014).

Accordingly, this project explored a number of technical options for improving NP measurement in the workplace and provided an opportunity to test them in the field. As an exhaustive presentation of NP types, their behaviour, related health and safety risks and risk management methods was recently provided in the best practices guidance mentioned above (Ostiguy et al., 2014), only a summary recap of the problems posed by these compounds is given here. The recap is followed by a review of NP sampling and characterization methods in the section entitled "State of the Science."

1.2 The growing field of nanotechnologies (NT)

The exceptional properties of ENMs are driving rapid growth in the field of nanotechnologies, currently a major social issue (Ostiguy et al., 2008). Despite a lack of traceability, it is estimated that more than 1,800 products containing ENMs are now commercially available (Vance et al., 2015). The industrial application of products and processes developed in the laboratory has led to a dramatic increase in the volume of ENMs handled and in the number of people possibly exposed to them (Ostiguy et al., 2008). A recent study mapping the use of nanotechnologies in

[1] http://www.irsst.qc.ca/publications-et-outils/publication/i/100663/n/caracterisation-etcontrole-de-exposition-professionnelle-aux-nanoparticules-et-particules-ultrafines-r-746

[2] http://www.irsst.qc.ca/media/documents/PubIRSST/R-899.pdf?v=2017-07-22; http://www.irsst.qc.ca/en/publications-tools/publication/i/100775/n/nanomateriaux-guide-r-840

Québec industries and research laboratories indicates that some laboratories and industries use more than one kilogram a year—particularly carbon black, carbon nanotubes (both single-walled, SWCNT, and multiwalled, MWCNT) graphene, aluminum, zinc and silicon oxides, nanoclays and nanocrystalline cellulose. Most establishments that use NPs are small to medium-sized enterprises with other industrial activities, and less than 10% of their activities use NPs—except in the case of companies that produce NPs (Endo, 2014).

1.3 Health risks

Animal studies demonstrate that ENMs show higher toxicity than an equivalent mass of their bulk counterparts. They can cause oxidative stress, inflammation, fibrosis, granuloma formation and circulatory system effects. These studies have also demonstrated that modifications to the chemical composition, crystalline structure and particle size of ENMs directly influence their biological impact (Ostiguy et al., 2008, 2010; Shvedova et al., 2012; Stone et al., 2010). These results are generating concern about the possible risks of occupational exposure to ENMs, through inhalation as well as dermal exposure (Monteiro-Riviere and Riviere, 2009; Ostiguy et al., 2008, 2010; Riviere et al., 2012; Saathoff et al., 2011; Schaeublin et al., 2012; van der Merwe et al., 2009). In terms of regulation, there are few exposure limit values available for gauging the risk to workers exposed to these compounds. This has led a number of organizations, including the IRSST, to suggest the use of the precautionary principle to minimize ENM exposure (AFSSET, 2008; NIOSH, 2011; Ostiguy et al., 2008, 2010, 2014).

1.4 Inadequacy of exposure measurements and monitoring

The monitoring of airborne ENM contamination levels remains a complex process. Challenges include i) the simultaneous presence of particles of nanometric size that are not ENMs; and ii) the diversity of the parameters to be measured (e.g., mass, number of particles, size, particle-size distribution, chemical composition, particle surface area and morphology).

To overcome the technical difficulties of sampling and characterizing airborne ENMs, new samplers designed for the collection of personal samples and their subsequent laboratory analysis are currently under development or in the workplace validation phase (Cena et al., 2015; Cena et al., 2014; Cena et al., 2011; Motellier et al., 2011). Methodological limitations in obtaining and interpreting sampling results have also been established: collection on filters, for example, can lead to the underestimation of the smallest particles (Johnson et al., 2010). Also, difficulties establishing the relation between aerodynamic diameter determined with selective samplers and physical diameter of the particles measured by microscopy have been reported (Noël et al., 2013). What's more, existing methods for estimating exposure to airborne ENMs, which essentially use direct-reading instruments, respond non-specifically to all airborne particles in the workplace.

Though a number of organizations are developing strategies to evaluate occupational exposure to airborne ENMs (Debia et al., 2012a; Kuhlbusch et al., 2011; NIOSH, 2009; Witschger et al., 2012), there has been little study of methods specifically for sampling surfaces—which could show presence of ENMs on work surfaces, equipment, skin or protective clothing. Some researchers and organizations, including the INRS and the IRSST, emphasize the need to sample

surfaces to control the presence of ENM deposits (Ostiguy, 2010; Ostiguy et al., 2014; Witschger et al., 2012; Woskie et al., 2010).

For all these reasons, the development and validation of more sophisticated methods of sampling and characterizing ENMs in the air and on work surfaces is crucial for a better understanding of the possible occupational health risks. This study was thus designed to determine the best way to estimate occupational exposure to ENMs by combining existing techniques.

2. STATE OF THE SCIENCE: REVIEW OF NP SAMPLING AND CHARACTERIZATION METHODS

Following is a review of the literature on methods currently used to evaluate occupational exposure to ENMs. At present, the quantification and characterization of occupational ENM exposure is carried out mainly with direct-reading instruments (DRI) (real-time as opposed to integrated measurements, which require subsequent laboratory analysis), by gravimetric or chemical analysis and/or by electron microscopy analysis of samples previously collected on different types of supports (Leskinen et al., 2012; NIOSH, 2009).

Different exposure measurement strategies are possible by combining these measurement techniques in different ways. The National Institute for Occupational Safety and Health (NIOSH, 2009), for example, suggests a two-step approach. The first step is preliminary measurements with a small number of DRIs and electron microscopy analysis (to confirm presence or absence of NPs). The second step is complete characterization requiring more specialized instrumentation and specific chemical analyses. The IRSST recommends that, at minimum, particle number concentration, particle-size distribution, specific surface and chemical composition be determined so that exposure, expressed as aerosol mass per particle-size fraction, can be established (Ostiguy et al., 2014).

2.1 Real-time measurement

Condensation particle counters (CPCs) and optical particle counters (OPC) can be used to determine ENM emissions by measuring particle number concentrations (number of particles/cm³). A number of field studies report use of these instruments to measure Fe, Ni, Al and Si particles (Baron et al., 2002; Fujitani and Kobayashi, 2008; Huang et al., 2012; Maynard et al., 2004; Methner et al., 2010a; NIOSH, 2009; Peters et al., 2009). A wider particle size range can be covered by using a CPC together with an OPC. CPCs generally measure number concentrations of particles with diameters ranging from a few dozen nanometres to more than 1,000 nm, whereas an OPC can generally measure number concentrations of particles with diameters ranging from 300 nm to 10,000 nm.

Light-scattering aerosol photometers, such as the DustTrak (TSI Inc.), can also be used to measure fine aerosols. Photometers measure mass concentrations and are widely used in occupational and environmental hygiene to measure dust in various environments—including offices, industrial workshops and outdoor environments (Bello et al., 2009; Bello et al., 2010; Evans et al., 2010; Nilsson et al., 2013; Raynor et al., 2012).

Other larger and more costly measuring instruments are also commonly used, including the following: scanning mobility particle sizers (SMPS); fast mobility particle sizers (FMPS); and electrical low-pressure impactors (ELPI). These devices provide both number and mass concentrations for different particle size fractions (Bello et al., 2010; Brouwer et al., 2013; Leskinen et al., 2012; Schlagenhauf et al., 2012). The particle-size distribution of an aerosol is, in fact, an essential parameter for characterizing nanoparticle health risk, as the site of deposit in the airways when ENMs are inhaled correlates closely with particle size (Ostiguy et al., 2014). These instruments can generally be used to measure concentrations of particles ranging in size

from a few nanometres to more than 500 nm (several micrometres), depending on the instrument. Table 1 summarizes the key characteristics of the DRIs described above.

Table 1 – DRIs: key characteristics and examples

Instrument	Description
Condensation particle counter (CPC)	Measures particle number concentration (particles/cm³) by detecting light scattered by individual particles. Particles are first grown by vapour (isopropanol or water) condensation to sizes large enough to be counted. Ex.: P-Trak 8525; TSI 3007 (TSI Inc.)
Optical particle counter (OPC)	Uses light-scattering technology to measure number of particles of various sizes per unit volume (particles/m^3). Ex.: Aerotrak 9306 (6 fractions); Model No. 3330 (16 fractions) (TSI Inc.)
Laser photometer	Measures aerosol mass concentration from light scattered from particles, calibrated against a standard test dust (Arizona Road Dust) Ex.: Dust-Trak DRX 8533 (TSI Inc.).
Electrical mobility spectrometer (SMPS and FMPS)	Measures particle size distribution of airborne particles as a function of electrical mobility diameter, determined using several electrometers with very low detection limits. Ex.: NanoScan SMPS 3910; FMPS 3091 (TSI Inc.)
Electrical low-pressure impactor (ELPI)	Measures particle size distribution and particle number concentration (particles/cm^3) as a function of aerodynamic diameter (12 particle size fractions).

The main limitation of these instruments stems from their non-specificity, that is, they react to all types of aerosols, irrespective of their composition: ENMs, ENM agglomerates, unintentionally released fine and ultrafine particles and background particles present in any work environment. Hence background measurement seems to be a crucial step in assessing ENM exposure with DRIs. It is thus recommended that concentrations before and after work be compared (or measurements taken when there is no work compared to measurements taken while work is in progress) (Dahm et al., 2012). Ratios (R) of concentrations measured during work processes (P) to that measured in the background (B) can be calculated as indices of the relative impact of the process (Cena and Peters, 2011).

2.2 Integrated measurement

Occupational exposure to ENMs can also be determined by laboratory analysis of samples first collected in a variety of ways. Possible laboratory analyses include i) characterization by transmission electron microscopy (TEM) or scanning electron microscopy (SEM); ii) thermal-optical elemental carbon (EC) analysis (NIOSH 5040) and iii) inductively coupled plasma mass spectrometry analysis (ICP-MS).

2.2.1 Electron microscopy characterization

2.2.1.1 Types of microscopy

Electron microscopy (EM) is decidedly the gold standard for confirming presence, shape and degree of agglomeration of NPs (Bello et al., 2009; Brouwer et al., 2013; Fleury et al., 2013; Lee et al., 2010; Peters et al., 2009; R'Mili et al., 2011; R'Mili et al., 2013; Schlagenhauf et al., 2012; Shepard and Brenner, 2014a; Van Landuyt et al., 2014; Vorbau et al., 2009). Scanning electron microscopy (SEM) and transmission electron microscopy (TEM) are commonly used to observe NPs. Observation quality generally depends on the performance of the microscope used and the diameter of the NPs, taking into account as well that resolution is generally higher with TEM than SEM. Both TEM and SEM generally work very well for observation of carbon nanotubes (CNTs) and carbon nanofibres (CNF), which are most often found highly agglomerated in workplaces (Baron et al., 2002; Bello et al., 2009; Huang et al., 2012; Maynard et al., 2007; Maynard et al., 2004; R'Mili et al., 2011; Schlagenhauf et al., 2012). Observation of individual CNT fibres, particularly the narrowest ones (SWCNT), is often more difficult with SEM.

For CNTs/CNFs, which include metal catalysts, electron microscopy observation can be coupled with elemental chemical analysis by energy-dispersive X-ray spectroscopy (EDS). EDS can be used to characterize metal NPs, and their presence in agglomerated form in personal breathing zones in the workplace has been confirmed in a number of cases reported in the literature (Koivisto et al., 2012; Lee et al., 2011; Sahu and Biswas, 2010; Shepard and Brenner, 2014b; Tsai et al., 2012; Tsai et al., 2009b).

2.2.1.2 Fibre counting

Counting of fibrous particles or structures containing fibrous particles is also mentioned in the literature in cases of possible exposure to CNTs and CNFs. In most of these studies, the NIOSH 7402 method (traditionally used to count asbestos fibres but eventually adapted) was employed to analyze the samples. All particles, or structures containing particles, with aspect ratios greater than 3:1 were counted in a representative number of randomly selected grid openings. Structure number concentration (CNT structures/cm³) is calculated from average counts, surface area of the count zones and sample volume. With respect to MWCNTs, 0.002 and 193.6 CNT structures/cm^3 were measured in the personal breathing zone of workers performing sonication (Dahm et al., 2013; Dahm et al., 2012) and composite-blending tasks, respectively (Han et al., 2008). As for SWCNTs, counts of 0.002 to 0.013 CNT structures/cm³ have been reported for SWCNT harvesting and reactor cleanout (Dahm et al., 2013; Dahm et al., 2012; Ogura et al., 2011).

2.2.1.3 Sample collection

The success of electron microscopy observation depends to a large extent on the methods of collecting NPs on the supports to be analyzed. The different sampling methods that can be used are discussed below.

2.2.1.3.1 Filter

Aerosol particles can be collected on a polycarbonate filter membrane with a fixed pore size and a sampling pump. As the polycarbonate membrane is not itself a conductor, it must be covered with a conductive coating (deposit of gold or platinum in vapour phase) before or after the particle sampling. This method was demonstrated to be effective in a study by Safe Work Australia involving SEM analysis of MWCNTs collected on a gold-coated polycarbonate membrane (100-nm pores) (Safe Work Australia, 2010).

2.2.1.3.2 Grid

Aerosol particles can be actively sampled, by aspiration, and collected by inertial impaction on a microscopy grid attached or taped to an impactor stage (Birch et al., 2011) or a filter membrane (Debia et al., 2012b; Ostiguy, 2014; Tsai et al., 2009a; Tsai et al., 2009b). If a multi-stage cascade impactor is used (such as an ELPI or a Sioutas [SKC, TSI Inc.]), the particles can be collected according to size, and each size class can be analyzed separately. A variety of pumps operating at high flow rates may be required to collect the aerosols and run them through these multi-stage devices. Tsai et al., on the other hand, recommend operating the sampler at a low sampling rate (0.3 L/min for a 47-mm cassette) to ensure the samples are not overloaded with particles that are too large and to increase residence time in the devices and hence enhance NP collection through Brownian movement (Tsai, 2013).

2.2.1.3.3 Mini Particle Sampler® (MPS)

A research group from France's national institute of industrial safety and environmental protection (INERIS) has developed an instrument specifically for collecting particles on TEM grids (R'Mili et al., 2013), the Mini Particle Sampler® (MPS). With the MPS, air collected in a worker's breathing zone passes through a porous TEM grid (Lacey, Holey or Quantifoil) (Figure 1). NPs are thus collected and deposited directly on the TEM observation grid, making it possible to collect high densities in a very short time. Collection efficiency of a Quantifoil-type porous TEM grid (hole diameter = 1.2 to 1.3 µm; hole density = 1.3×10^7 pores/cm^2; flow rate = 0.3 L/min) for nanoparticles 5 to 150 nm in size ranged from 15 to 70%, with minimum efficiency at around 30 nm (R'Mili et al., 2013).

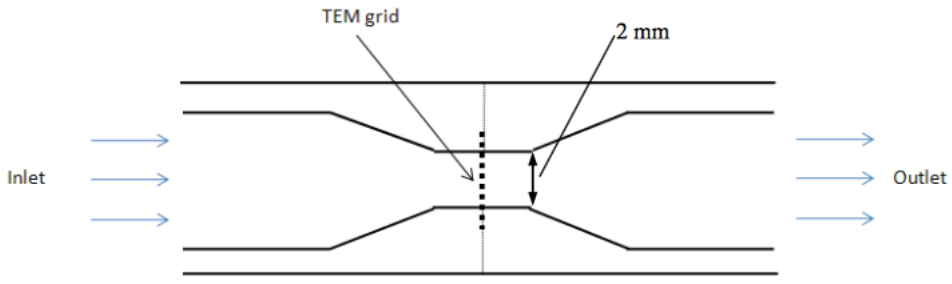

Figure 1 – Concept diagram, Mini Particle Sampler® (MPS) (R'Mili et al., 2013)

2.2.1.3.4 Other techniques

Other methods of NP collection are also described in the literature, including one using an electrostatic filter (Bello et al., 2008; Ku et al., 2007) and another using thermophoretic repulsion (Bello et al., 2008; R'Mili et al., 2011). Electrical discharge is used to collect particles on a TEM grid in the first case and a thermal gradient in the second.

Some researchers have used a modified version of NIOSH 7402, traditionally used to sample and quantify asbestos fibres. This method makes use of a filter that can be dissolved after particle collection and before particle transfer onto a TEM grid for subsequent analysis (Dahm et al., 2012; Han et al., 2008; Methner et al., 2010a).

Lastly, surface sampling methods can also be used to sample a work environment. A microvacuum or wet cloth is used to collect nanoparticles present on work surfaces. The particles are then transferred onto a TEM grid for subsequent qualitative microscopy analysis (ASTM, 2014).

2.2.2 Measurement of elemental carbon (EC)

Originally developed to estimate exposure from diesel engine emissions (NIOSH, 2003), the NIOSH 5040 method for measuring elemental carbon is currently suggested for measuring occupational exposure to CNTs and CNFs and is recognized as specific and reliable (Birch et al., 2011; NIOSH, 2003, 2013; Ono-Ogasawara and Myojo, 2011). The method has been used in a variety of studies of industrial facilities that use CNTs and CNFs. As for exposure to MWCNTs, EC concentrations between 0.5 µg/m³ and 48 µg/m^3 have been measured in worker breathing zones. The lowest values were recorded during sanding of composites containing MWCNTs (Heitbrink et al., 2013) and the highest when handling powders (Ono-Ogasawara et al., 2013). As for SWCNT exposure, the lowest EC concentrations recorded in worker breathing zones were below detectable threshold, during sonication (Lo et al., 2013) as well as handling and cleaning procedures (Methner et al., 2012a). EC concentrations as high as 38 µg/m³ were recorded when harvesting SWCNTs from a reactor (Methner et al., 2012a). With CNFs as well, EC concentrations recorded in the breathing zone were below detectable levels during weighing of raw nanomaterial powder and sanding of composites containing CNFs (Methner et al., 2012a; Methner et al., 2012b), though concentrations as high as 1,000 µg/m³ are reported during wet cutting of composites containing CNFs (Methner et al., 2012b).

Use of Sioutas cascade impactors or micro-orifice uniform-deposit impactors (MOUDIs) is also mentioned in the literature on EC measurement, specifically with different particle size fractions (Birch et al., 2011; Ono-Ogasawara and Myojo, 2011).

2.2.3 Measurement by inductively coupled plasma mass spectrometry (ICP-MS)

One suggested alternative to EC measurement for assessing occupational exposure to CNTs and CNFs is to use ICP-MS to detect catalytic metals (Birch et al., 2011; Maynard et al., 2004; Rasmussen et al., 2013; R'Mili et al., 2011; Reed et al., 2013). The quantity of ENMs is then

estimated from the metal content measured in the samples. However, characterization of the raw material is often required for this method to be applicable. Furthermore, Birch et al. reported major limitations with this approach, including detection of metals unrelated to CNFs and detection limits that are often too high to identify low-level exposure (Birch et al., 2011).

A number of authors report using different methods to collect samples on filters that are subsequently analyzed by ICP-MS to quantify exposure to metal oxides. Aluminum oxide concentrations in a worker's breathing zone can be as high as 157 µg/m³ during reactor cleanout tasks after production of aluminum oxide nanoparticles (Methner et al., 2010a). Berges et al. (2007) estimated that concentrations of titanium dioxide in the breathing zone of a worker bagging TiO_2 ranged from 10 µg/m³ to 150 µg/m³ (Berges et al., 2007). Also reported are silver concentrations between 0.09 µg/m³ (Lee et al., 2012; Lee et al., 2011) and 33 µg/m³ (Methner et al., 2010a) during manufacturing processes and reactor cleanout, respectively, following nano-sized silver production. Lastly, iron concentrations of 32 µg/m³ to 335 µg/m³ are reported by Methner et al. (2010) during reactor cleanout with and without exposure control measures (Methner et al., 2010a).

3. RESEARCH OBJECTIVES

3.1 General objective

The purpose of this project was to develop innovative methodological approaches for sampling and quantitative and/or qualitative characterization of specific ENMs in the air and on surfaces in the workplace.

3.2 Specific objectives

Based on the review of existing methods presented in Section 2 above, the specific objectives of this project were as follows:

- Compare different sampling devices and analysis techniques, taking into consideration the various characteristics of ENMs and other exposure parameters (e.g., size, concentrations and exposure duration)

- Contribute to the development of standard methods of ENM collection and characterization as well as the development of new ways of doing things and the implementation of innovative strategies

- Evaluate and document levels of exposure to ENMs in the air and on surfaces (floor, work surfaces and instruments) in a variety of work environments by implementing the strategies mentioned above

4. METHODOLOGY

There are two complementary parts to the project: a laboratory investigation (Part A) and a fieldwork component (Part B). Part A consisted in examining different collection and analysis devices during TiO_2 generation under controlled laboratory conditions. Part B consisted in a series of field studies tailored to particular work environments and designed to test a variety of devices and analysis procedures and to measure occupational exposure levels.

These two parts of the project are described in more detail below, but first, the instrumentation, sampling protocols and analytical methods are described.

4.1 Methods and equipment

Instrumentation for the project was assured by the occupational hygiene laboratory of the Université de Montréal's school of public health (ESPUM), the IRSST, Polytechnique Montréal's centre for microscopic characterization of materials (CM^2) and ESPUM's biomarkers and nanoparticles analysis unit. Each laboratory was also responsible for the required calibration of the different devices.

4.1.1 Real-time measurements – direct-reading instruments (DRIs)

Table 2 shows the different DRIs used for our investigations. Unless indicated otherwise and in the absence of measurement alternatives, priority was given to "personal measurements," that is, measurements taken as close as possible to the worker's breathing zone. To do this, workers were monitored by one of our researchers using instruments fitted with Tygon® sampling probes. The DRIs used were placed on a mobile platform, in an arrangement similar to that shown in Figure 2. Measurements were taken at ten-second intervals for the duration of the work task.

Table 2 – Direct-reading instruments (DRIs) used for aerosol characterization

Model	Type of instrument	Parameter measured (concentration unit)	Size of particles measured (nm)
P-Trak 8525 (TSI Inc.)	Condensation particle counter (CPC)	Number concentration (#/cm^3)	20 – 1,000
AeroTrak 9000 (TSI Inc.)	Battery-operated diffusion charger	Specific surface area of alveolar fraction (µm^2/cm^3)	10 – 1,000
AeroTrak 9306 (TSI Inc.)	Optical particle counter (OPC)	Number concentration (#/cm^3) for six size fractions (0.3 µm, 0.5 µm, 1 µm, 3 µm, 5 µm and 10 µm)	300 – 10,000
DustTrak DRX 8533 (TSI Inc.)	Laser photometer	Mass concentration (mg/m^3) for four size fractions (PM_1, $PM_{2.5}$, $PM_{respirable}$ and PM_{10})	100 – 15,000
EEPS 3090 (TSI Inc.)	Spectrometer	Electrical mobility diameter Particle size distribution Number concentration (#/cm^3) for 32 size fractions	56 - 560
ELPI (Dekati)	Electrical low-pressure impactor	Aerodynamic diameter Particle size distribution Total number concentration (#/cm^3) for 12 size fractions	24 – 6,700

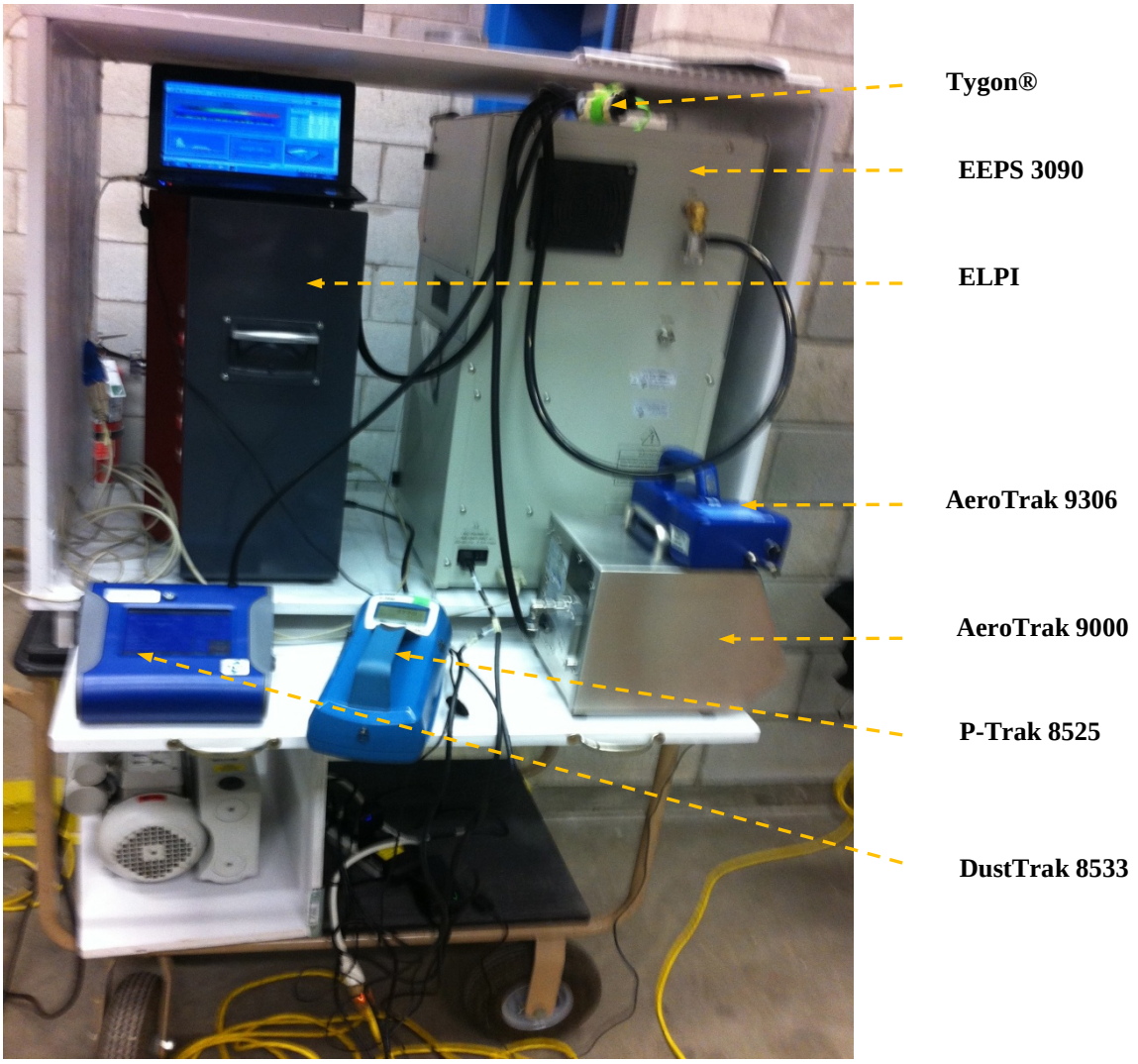

Figure 2 – Assembly of direct-reading instruments (DRIs)

4.1.2 Integrated measurement – analyses of deposits on collection media

4.1.2.1 Electron microscopy

4.1.2.1.1 Electron microscopy analysis systems

4.1.2.1.1.1 Scanning electron microscopy (SEM)

Scanning electron microscopy (SEM) can be used to examine size, number, morphology and elemental composition of particles collected on a microscopy grid. For this project, a JEOL JSM-7600F field emission gun scanning electron microscope (FEG-SEM) operating at 0.1 to 30 kV was used. This microscope has two spectrometers for detecting x-rays, one an energy dispersive

spectrometer (EDS) and the other a wave-dispersive spectrometer (WDS). The microscope also incorporates two secondary electron detectors, two backscattered electron detectors and a detector for transmitted electrons (STEM detector).

4.1.2.1.1.2 Transmission electron microscopy (TEM)

Transmission electron microscopy (TEM) can be used to examine size, number, morphology and elemental composition of particles collected on a microscopy grid. For this project, a JEOL JEM-2100F field emission gun transmission electron microscope (FEG-TEM) operating at 200 kV was used. The microscope is equipped with an energy-dispersive x-ray spectrometer and an electron energy loss spectrometer (EELS). It also has two digital cameras.

4.1.2.1.2 SEM/TEM sampling device

For this project, particles were collected directly on microscopy grids to avoid handling of the samples. Several types of copper grids 3 mm in diameter were used for NP collection. Most were conventional copper grids covered with a continuous carbon film (that is, without holes), the grid having 200 or 400 openings per inch (200 or 400 mesh, Agar Scientific). Index grids (Figure 3) with holey films were also used (Quantifoil® 1.2/1.3 H7, Agar Scientific). The index feature enables the position of each grid square analyzed to be referenced and identified. Index grids can be used in TEM or SEM analyses.

Different devices and procedures were used to collect particles on the grids:

- A three-piece, 37-mm, 2.0-µm cassette with polytetrafluorethylene (PTFE or Teflon) filter. The grids were glued directly to the filter with commercial glue. Air was then drawn through the cassette with a GilAir (Gilian®) or AirLite® (SKC, Inc.) pump at a flow rate of 1.5 to 2.5 L/min.

- The Mini Particle Sampler® (MPS) developed by INERIS and described above in Section 2.2.1.3.3 (Figure 1). With the help of a GilAir® pump, air was drawn into the sampler at a flow rate of 0.3 L/min and sent through a porous microscopy grid (Quantifoil® 1.2/1.3, H7, Agar Scientific). These grids were covered with a carbon film with holes about every 1.3 µm and 400 openings per inch (400 mesh) to provide good support for the film.

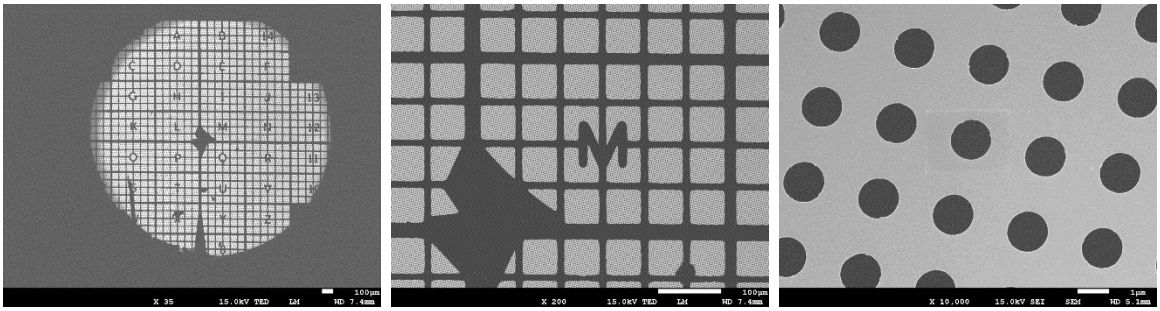

Figure 3 – Index grid covered with holey film

4.1.2.1.3 SEM/TEM analysis

4.1.2.1.3.1 Determining the number of SEM/TEM observations required

Each stereological parameter of interest was measured for each object present in each field characterized. As each field was characterized, a graphic representation of the mean value of the measured parameter was plotted for each field (fields 1, 2, 3, 4, 5, etc. on the *x* access) (see Figure 4). The figure thus generated shows the variation in the parameter of interest from one field to the next. At the same time, the cumulative mean calculated for the growing number of fields is also plotted on the figure. Thus, for the first field, the value of this cumulative mean will obviously be equal to the value of the parameter measured for the first field, as there is only a single value at this point. For the second field, however, the cumulative mean will be the mean of the measurements for the parameter of interest obtained for the first and the second field, and the cumulative value plotted for the third field will be the average for the first three fields. At first, the cumulative mean varies more or less as a function of the growing number of fields, but with a sufficient number of fields, it eventually stabilizes and plateaus. The number of fields before the start of the plateau is the number of fields required to obtain an average of the stereological parameter of interest deemed representative of the sample (stable value).

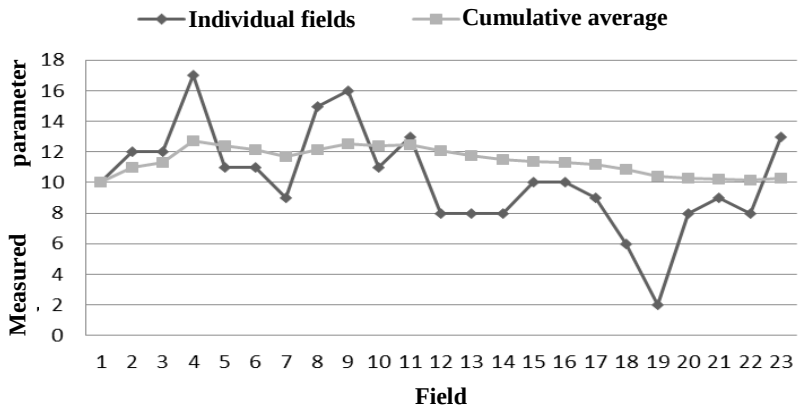

Figure 4 – Sample plot for determining number of fields to view for microscopy analysis

4.1.2.1.3.2 SEM/TEM image processing

The first step is to open the image in an image analysis software and to calibrate it according to the magnification used during acquisition (Figure 5a). The second and most important step is grayscale thresholding to select the objects one wants to measure. As grayscale thresholding sometimes leaves unselected areas within objects, a manual fill operation is required. A disconnection operation is then performed to separate particles that are touching but do not seem to be agglomerated (Figure 5b). A cleaning operation is then launched to erase all regions selected during the grayscale thresholding that are not part of the objects to be measured. Lastly, a filling and manual cleaning operation is performed to ensure that all objects that must be measured have been correctly selected (Figure 5c).

The parameters measured by the image analysis software were as follows:

- Internal diameter: the diameter of the largest circle that can be inserted in its entirety inside the object

- External diameter: the diameter of the smallest circle within which the object can be inserted

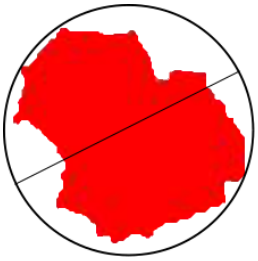

- Circular diameter: the diameter of a circle of the same area as the object

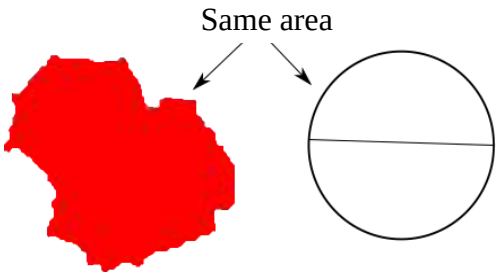

The surface area occupied by the particles is calculated by multiplying the average area of a sphere ($4\pi R^2$) by the number of particles counted in a determined number of fields.

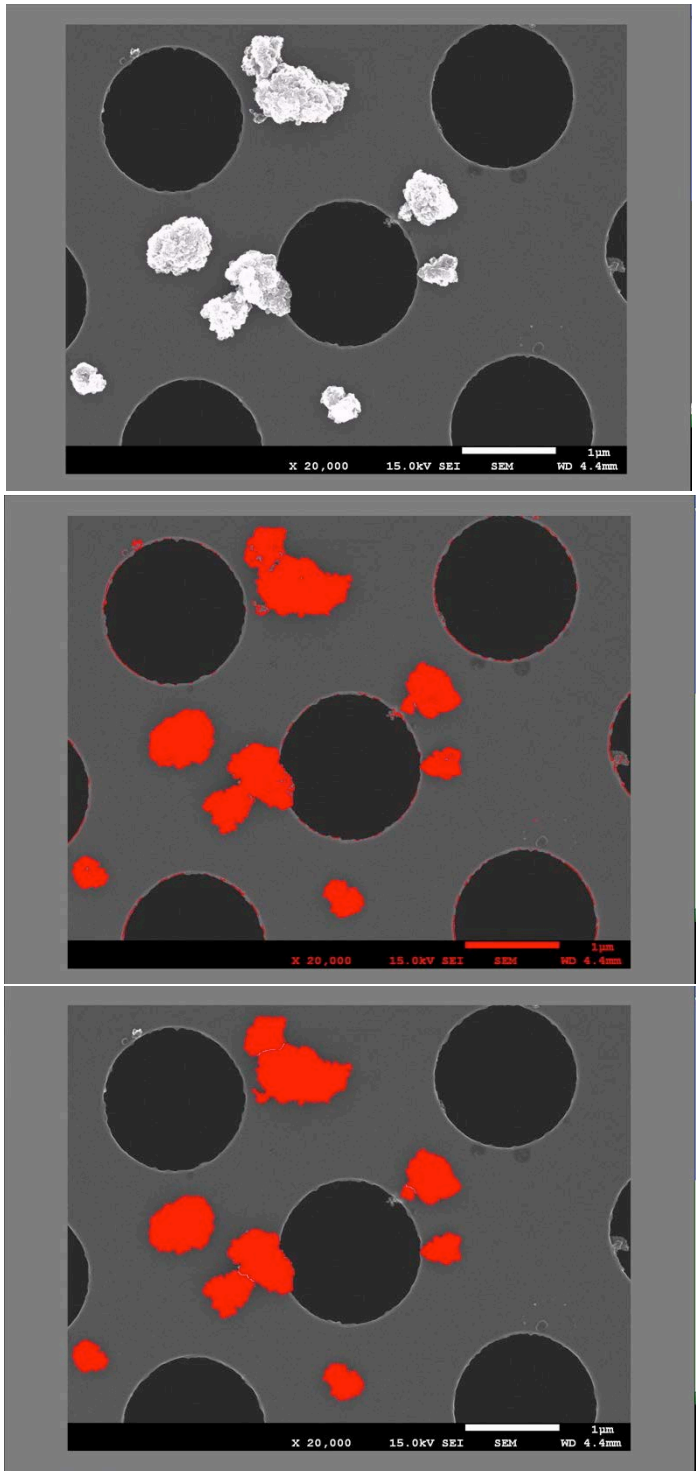

Figure 5 – Main steps in image analysis

4.1.2.2 Elemental carbon (EC) measurement

Three different sampling techniques were used to measure elemental carbon (EC). The first applies NIOSH recommendations (NIOSH 5040) using 3-piece, 37-mm cassettes (SKC Inc.) with quartz-fibre filters together with a GK 2.69 cyclone (BGI, Inc.), making it possible to collect the respirable aerosol fraction only. The GilAir® pumps used for this sampling method were adjusted to a flow rate of 4.2 L/min. The two other techniques tested used SKC personal parallel particle impactors (PPI), once again with quartz-fibre filters. Legacy pumps (SKC, Inc. Cat No. 100-3000) and AirLite® pumps adjusted to 8 and 2 L/min respectively were used to sample respirable and thoracic aerosol fractions. Measurements were taken in the workers' breathing zone for the duration of their tasks (Figure 6).

Figure 6 – Arrangement of personal sampling devices on a worker.

The analysis method used, based on thermal-optical analysis, is described by the NIOSH method 5040. The analyses were conducted by Galson Laboratories, accredited by the American Industrial Hygiene Association (AIHA) - Laboratory Accreditation Programs (AIHA-LAP) (ISO 17025).

4.1.2.3 Gravimetric measurement

The IRSST method 48-1 was applied to measure mass concentrations of respirable aerosol fractions. Three-piece, 37-mm cassettes with polyvinyl chloride (PVC) filters coupled with GS3 cyclones and pumps set to a flow rate of 2.75 L/min were used. The analyses were performed in the IRSST laboratories, accredited by the AIHA Laboratory Accreditation Programs (AIHA-LAP) (ISO 17025).

4.1.2.4 Raman spectroscopy measurement

Raman spectroscopy analyses (inVia, Renishaw) were performed to characterize CNTs. This characterization technique relies on scattering of monochromatic light from a laser projected onto the sample to be analyzed. In this study, copper microscopy grids served as the substrate

onto which the Raman analyses were performed. Calibration tests were performed to determine reference signals with an intact grid, a grid containing carbon black and a grid containing CNTs (SWCNTs). The tests were performed at wavelengths of 514 nm (Argon gas laser), 633 nm (He-Ne gas laser) and 785 nm (diode laser) to determine the best signal-to-noise ratio (SNR) and thus the optimal laser wavelength. To validate the presence of CNTs in the samples, the different spectra were compared to reference spectra.

4.1.2.5 Measurement by inductively coupled plasma mass spectrometry (ICP-MS)

ICP-MS analyses were performed to determine TiO_2 concentrations. ICP-MS measurement relies on separation, identification and quantification of the constituent elements of a liquid sample (or a sample rendered liquid) based on mass-to-charge ratio (m/z). Particles are collected on 37-mm, 0.8-µm mixed cellulose ester (MCE) filters using a sampling pump. The MCE filters are digested on a hot block at 135°C in a mixture of nitric acid, hydrogen peroxide and hydrofluoric acid to obtain a homogenous liquid mix. An indium (In) internal standard is added to the sample using the method developed by the ESPUM's biomarkers and nanoparticles analysis unit (personal communication, Michèle Bouchard). ICP-MS is calibrated and optimized daily prior to analysis using a 1-ppb standard solution composed of elements of low, medium and high mass (atomic mass of different isotopes: lithium (Li) 7, cobalt (Co) 59, yttrium (Y) 89, thallium (Tl) 205). The sample is analyzed after determination of a five-point calibration curve (0, 0.05, 0.5, 5 and 50 ppb). Table 3 shows the ICP-MS analytical parameters used.

Table 3 – ICP-MS analytical parameters (Université de Montréal)

Plasma power	1550 W
Distance between torch and sampler cone	10 mm
Carrier gas flow	0.65 L/min
Sample load speed	0.10 rps*
Integration time	2 s
Sample uptake time	75 s
Sample uptake speed	0.5 rps
Reaction gas (helium) flow rate	4.5 L/min

*Revolutions per second

4.1.3 Surface sampling protocol

Three surface sampling techniques were used for this project:

- Active sampling using a cassette with a 37-mm PTFE filter glued to a microscopy grid, a Gast pump and a flow rate of 2.5 L/min on a 30 cm x 30 cm (900 cm²) surface over two minutes (Figure 7). A flexible, disposable Tygon® sampling probe was attached to the end of the cassette and the surfaces were sampled in an overlapping "S" or "Z" pattern (ASTM, 2008).
- Passive collection (deposition/diffusion) on aluminum microscopy grid holders (Figure 8) designed specifically for this project and placed perpendicular to the floor in different workplace locations.
- Wiping of 100 cm^2 with a wet MCE filter (SOP-00006 method) using a 10 cm x 10 cm template designed for ICP-MS TiO_2 analysis.

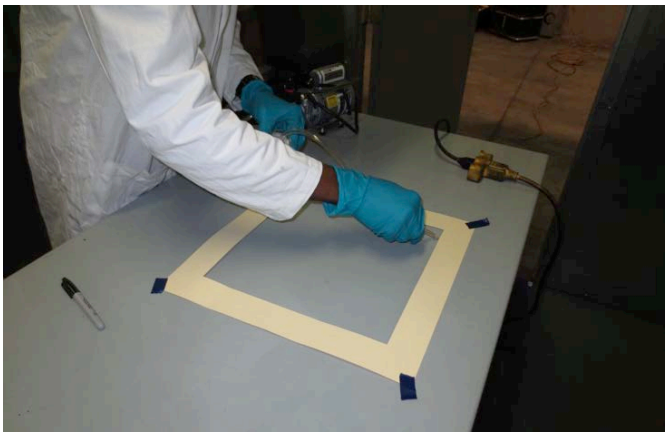

Figure 7 – Surface sampling on a table in an NP production room

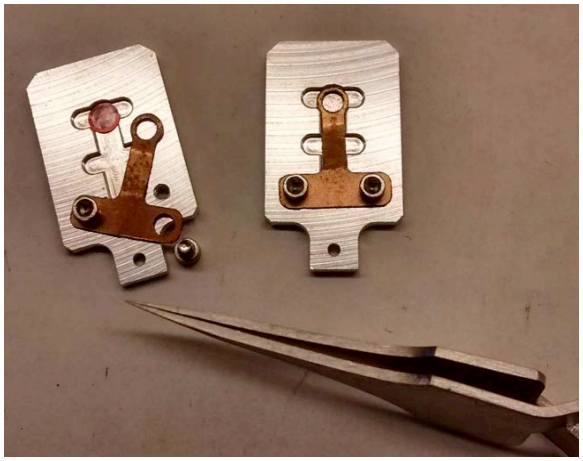

Figure 8 – Aluminum microscopy grid holder

4.2 Laboratory investigations: Part A

The first part of the project comprised a series of tests in an inhalation chamber to demonstrate the relative efficacy of the different collection devices and the possibilities for characterizing exposure based on the samples collected.

The "nose-only" inhalation chamber has an NP inhalation system with a Collision 6-jet nebulizer. Titanium dioxide (TiO_2) NPs were used for these tests. NPs with unit sizes of 7 nm (T1) and 50 nm (T2) were generated at concentrations of 1 mg/m^3. NP sampling times were 5 (D1), 10 (D2) and 20 (D3) minutes.

Concentrations were controlled with a combination of gravimetric measurements and direct readings using a laser photometer (DustTrak 8520). An SMPS was also used for real-time monitoring. For this part of the project, a number of measurements were taken simultaneously in the chamber in addition to the usual measurements:

- Collection on filtering microscopy grids in an MPS (GilAir® 5 pump, flow rate of 0.3 L/min)
- Collection on solid microscopy grids in a 37-mm cassette with PVC filter (GilAir® 5 pump, flow rate of 1.5 L/min)

4.3 Fieldwork: Part B

The second part of the project consisted in measuring different ENM exposure indicators in diverse work environments to test the methods available and the different strategies and to document contamination levels.

The field studies included i) real-time measurement of different parameters that can be measured using the DRIs described in Section 4.1.1; ii) collection of samples for qualitative and/or quantitative characterization of aerosols released in the workplaces, using the methods described in Section 4.1.2; and in some cases, iii) surface sampling and subsequent electron microscopy or ICP-MS analysis.

4.3.1 Description of work environments studied

In each workplace, the focus was mainly on tasks presumed to generate NPs and hence presenting the greatest exposure risk for workers. Table 4 summarizes the characteristics of the nine worksites visited (S1 to S9) and the activities or tasks investigated.

Table 4 – Worksites and work activities/tasks investigated

Site	Type of NP	Category	Description of activities	
S1	SWCNTs	P	Activity 1	Weighing of raw powders
			Activity 2	Mixing and homogenization
			Activity 3	Transfer and reaction
			Activity 4	Harvesting and cleanout
			Activity 5	Bagging of composite material
S2	Nanocrystalline cellulose	P	Activity 1	Shredding
			Activity 2	Drying and bagging
S3	Copper nanometals	P	Activity 1	Cleaning – opening tank, harvesting and screening (plant 1)
			Activity 2	Cleaning – removal and bagging of candles and dry cleaning of candle filter (plant 1)
			Activity 3	Cleaning – wet cleaning of candle filter (plant 1)
			Activity 4	Cleaning – washing candles (plant 1) with high-pressure water (plant 2)
			Activity 5	Cleaning – removal and bagging of candles and dry cleaning of candle filter (plant 2)
S4	CNFs, lithium iron phosphate, titanates	I	Activity 1	Weighing
			Activity 2	Transferring and reaction
			Activity 3	Harvesting and cleanout
S5	Zinc NPs	I	Activity 1	Ink flow test
S6	MWCNTs	I	Activity 1	Weighing
			Activity 2	Rheology testing
			Activity 3	Homogenization
			Activity 4	Transferring
			Activity 5	Sawing
			Activity 6	Sanding
			Activity 7	Dynamic Mechanical Analysis
S7	MWCNTs + nanoclays	I	Activity 1	Cutting
			Activity 2	Sanding
S8	TiO_2 + SiO_2	I	Activity	Varnishing
S9	Nanocellulose	P	Activity 1	Screening of shredded chips
			Activity 2	Digestion
			Activity 3	Functionalization (washing, filtering and drying)
			Activity 4	Grinding
			Activity 5	Screening and weighing functionalized NPs
			Activity 6	Screening and weighing nonfunctionalized NPs

P: producer; I: integrator

4.3.2 Field study program

Table 5 shows the field study program implemented to determine ENM exposure in the nine workplaces (S1 to S9) investigated.

Table 5 – Field study program at sites visited

Site	Aerosol characterization			Surface sampling
	DRIs	SEM/TEM	Other analyses	
S1	X	F, MPS	EC (Fr, Fth), Raman	F
S2	X	F		
S3	X	F		
S4	X	F		SEM-TEM/EDS(F) ICP-MS
S5	X	F		
S6	X	F		
S7	X	F		
S8	X	F, MPS	ICP-MS	SEM-TEM/EDS(F) SEM-TEM/EDS(GH)
S9	X	F		

F = Filter; MPS = Mini Particle Sampler®; GH = grid holder

EC = Elemental carbon; Fr = Respirable fraction; Fth = Thoracic fraction

When taking these measurements on site, all good industrial hygiene sampling practices were followed: preventive maintenance of equipment, calibration according to manufacturers' requirements, pump flow rate measurement before and after sampling, zero verification and use of control cassettes.

DRIs were used at all worksites investigated. Background concentrations were systematically measured with the DRIs before the beginning of work tasks to be evaluated.

Samples were collected for microscopy analyses with grids glued to a filter at nine sites. The MPS was used at sites S1 and S8.

Elemental carbon analyses were performed at site S1 using Raman spectroscopy and at site S8 using ICP-MS.

Surface samples were collected with a sampling pump and by wiping with a moist filter at sites S1 and S8. Lastly, grid holders were used to sample deposited particles at site S8.

5. RESULTS

5.1 Laboratory investigations: Part A

Tables 6 to 8 show results obtained using the image analysis technique described in Section 4.1.2.1.3.2. The number of fields assessed was the same for each grid (5, 10 and 20 minutes), that is, 30 fields (864 µm²).

Table 6 – Mean values obtained with image analysis for TiO_2 generation (7 nm, 1 mg/m³) and filtering grid/MPS sampling

	Internal diameter (µm)	External diameter (µm)	Circular diameter (µm)	Number of particles analyzed
5 minutes	0.24	0.52	0.38	578
10 minutes	0.27	0.54	0.41	440
20 minutes	0.26	0.60	0.43	527

Table 7 – Mean values obtained with image analysis for TiO_2 generation (50 nm, 1 mg/m³) and filtering grid/MPS sampling

	Internal diameter (µm)	External diameter (µm)	Circular diameter (µm)	Number of particles analyzed
5 minutes	0.15	0.38	0.27	264
10 minutes	0.24	0.57	0.41	281
20 minutes	0.28	0.65	0.48	293

Table 8 – Mean values obtained with image analysis for TiO_2 generation (7 nm, 1 mg/m³) and sampling with grids glued to filters

	Internal diameter (µm)	External diameter (µm)	Circular diameter (µm)	Number of particles analyzed
5 minutes	0.27	0.61	0.45	224
10 minutes	0.47	1.40	0.94	566
20 minutes	0.42	1.16	0.80	451

No marked increases in number of particles over time were noted, but average particle size practically doubled between 5 and 20 minutes (Table 7 and Table 8). These results suggest agglomeration on the microscopy grids.

Figure 9, Figure 10 and Figure 11 show the surfaces occupied by the particles in the 30 fields measured as a function of sampling time for each of the three grids analyzed. In all cases, no matter what type of diameter was measured, no linear relationship was noted. These results suggest overexposure of certain particles due to saturation of the grid. In the case of the 7-nm particles collected with the MPS, saturation seems to already have been reached at minute 5. Note as well that the image analysis method seems to be less effective with the 7-nm particles, once again suggesting limits associated with number of particles. Figure 12 shows the completely saturated microscopy grids obtained in the TiO_2 tests at a concentration of 5 mg/m^3. Because of the saturation, image analysis of these grids was impossible.

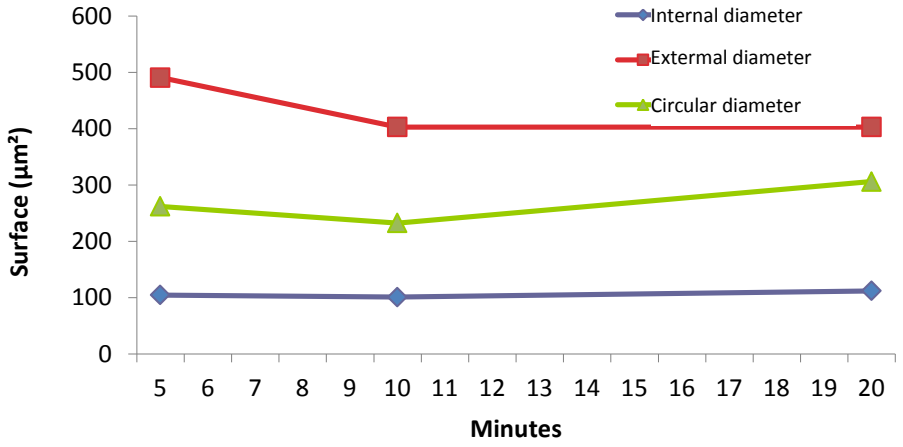

Figure 9 – Surface occupied by particles in the 30 fields investigated (7 nm, filtering grid/MPS)

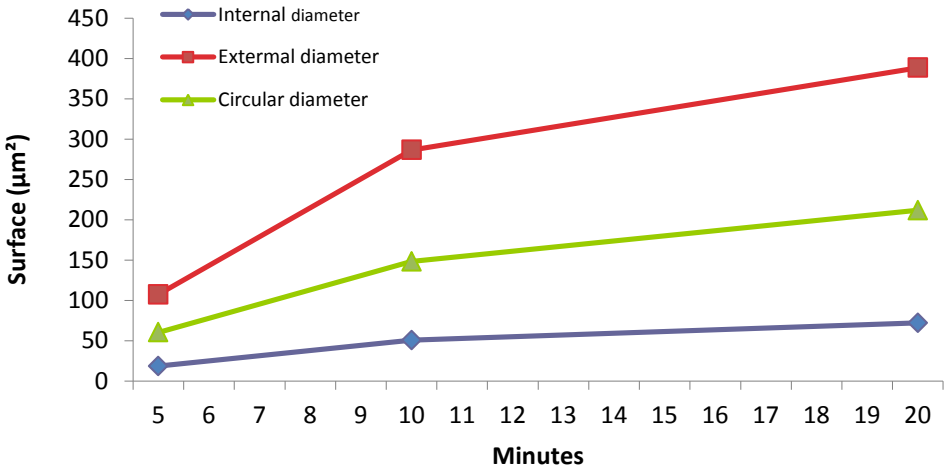

Figure 10 – Surface occupied by particles in the 30 fields investigated (50 nm, filtering grid/MPS)

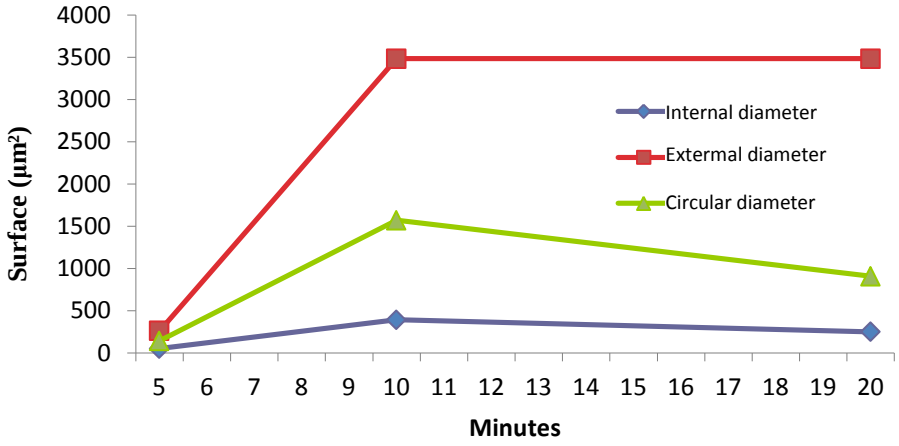

Figure 11 – Surface occupied by particles in the 30 fields investigated (7 nm, solid grid/filter)

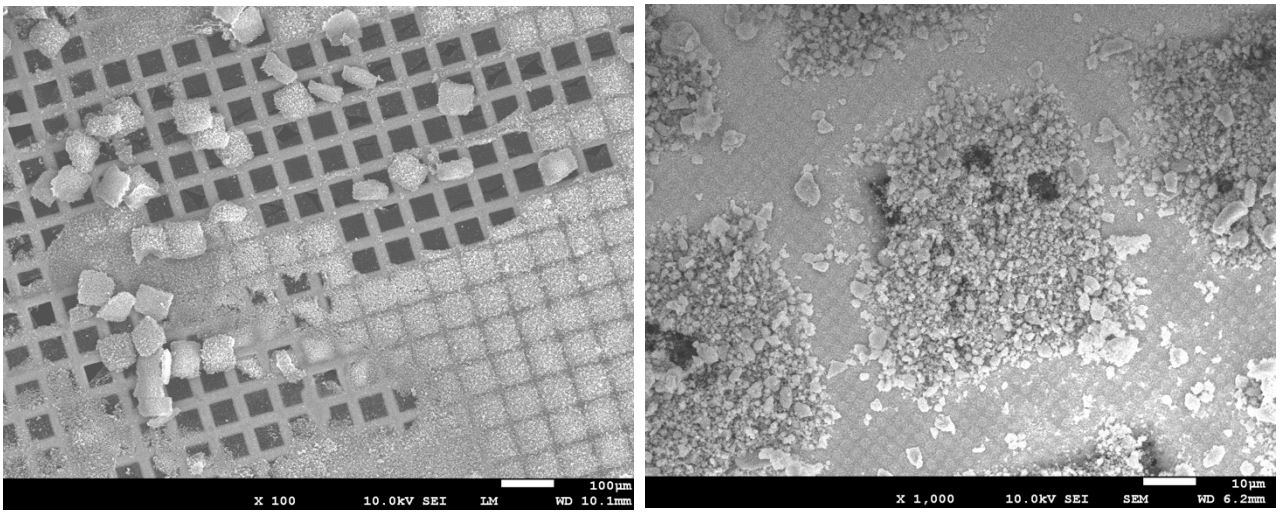

Figure 12 – TiO_2-saturated microscopy grids

5.2 FIELDWORK: Part B

5.2.1 Aerosol characterization

5.2.1.1 Number, mass and specific surface concentrations (DRIs)

Tables 9 to 17 show the different exposure concentrations measured with the P-Trak, the AeroTrak 9000 and 9306, and the DustTrak during the field studies for Part B of the project.

Site S1 (Table 9) –The DustTrak DRX detected a significant increase in particle number concentrations during activity 3 (transfer and reaction) and activity 4 (harvesting and cleanout) of the ENM production at this worksite. However, it must be considered that SWCNTs are

present only during activity 4 (cleanout), after synthesis, whereas in activity 3 (transfer), particles of carbon black and other metals are used.

Site S2 (Table 10) – A marked increase in concentrations was noted during activity 2 (drying and bagging), but only with the DustTrak DRX and the AeroTrak 9306. The two other instruments remained insensitive to nanocrystalline cellulose agglomerates.

Site S3 (Table 11) – Activity 3 and, to a lesser extent, activity 2 (both involving cleaning, wet and dry, respectively, of a candle filter used in the production of copper nanometals) resulted in increased emission of airborne particles. The increase was clearly detected with the DustTrak DRX and both AeroTrak models but was less evident with the P-Trak, again a sign of release of agglomerates.

Site S4 (Table 12) – The DustTrak DRX and the AeroTrak 9306, but not the P-Trak or the AeroTrak 9000, detected increases in concentrations during activity 2 (transfer and reaction) and activity 3 (harvesting and cleanout) in connection with the mechanofusion performed at this worksite. The increases were clearer with mix B (titanates) than with mix A (lithium iron phosphate).

Site S5 (Table 13) – The measuring devices all showed increased particle emissions during the activity investigated. At this site, the P-Trak increase ratios were comparable to those recorded with the other instruments, an indication that fine and ultrafine particles were generated.

Site S6 (Table 14) – Increase ratios were high for activity 3 (homogenization of a mixture on a hot plate) and activity 7 (DMA) with the P-Trak and the AeroTrak 9000. The results also indicate generation of aerosols during activity 6 (sanding). Only the P-Trak indicated a significant increase compared to background concentrations during activity 5 (sawing), though some increase seems to be suggested by the measurements taken by the other DRIs.

Site S7 (Table 15) – Comparison of activities 2 and 4, which use a ventilation table, with activities 1 and 3 (the same as activities 2 and 4, but without ventilation) clearly demonstrates that the table is effective in trapping aerosols generated. The very high ratios recorded with all measuring devices during activity 1 (cutting) are even higher than those recorded during activity 3 (sanding), which generates more dust.

Site S8 (Table 16) – Systematic calculation of high ratios with all DRIs used at this site indicates emission of aerosols composed of both fine particles and other agglomerates.

Site S9 (Table 17) – As at site S2 (also produces nanocellulose), the P-Trak could not detect increases in emissions, which were nonetheless clearly measured by the DustTrak DRX during activities 2, 4 and 6. Only the AeroTrak 9306 also showed these increases for particles ≥ 1 μm.

Table 9 – Mean number, mass and surface (per alveolar fraction) concentrations measured with DRIs during different tasks performed by workers at site S1

S1 – 1 to 3		Activity 1			Activity 2			Activity 3 [1]		
Instrument		BG	T	R	BG	T	R	BG	T	R
Number concentration (particles/cm³)*										
P-Trak		7,509	7,933	1.06	6,864	7,026	1.02	[7,472-13,115]	[11,058-15,369]	[1.17-1.48]
AeroTrak 9306	0.3 µm	-	-	-	-	-		-	-	-
	0.5 µm	-	-	-	-	-		-	-	-
	1 µm	-	-	-	-	-		-	-	-
	3 µm	-	-	-	-	-		-	-	-
	5 µm	-	-	-	-	-		-	-	-
	10 µm	-	-	-	-	-		-	-	-
Surface concentration (µm²/cm³) per alveolar fraction*										
AeroTrak 9000		33.3	35.57	1.07	43.14	42.49	0.98	[53.37-69.68]	[93-119.61]	[1.72-1.78]
Mass concentration (mg/m³)*										
DustTrak DRX	PM_1	-	-	-	-	-	-	-	-	-
	$PM_{2.5}$	-	-	-	-	-	-	-	-	-
	PM_{resp}	40	58	1.45	68	66	0.97	[89-113]	[253-275]	[2.24-3.13]
	PM_{10}	-	-	-	-	-	-	-	-	-
	PM_{total}	-	-	-	-	-	-	-	-	-

S1 – 4 to 5		Activity 4[1]			Activity 5		
Instrument		BG	T	R	BG	T	R
Number concentration (particles/cm³)*							
P-Trak		[9,633-11802]	[9,871-11,421]	[0.97-1.02]	9,689	9,536	0.98
AeroTrak 9306	0.3 µm	-	-	-	-	-	-
	0.5 µm	-	-	-	-	-	-
	1 µm	-	-	-	-	-	-
	3 µm	-	-	-	-	-	-
	5 µm	-	-	-	-	-	-
	10 µm	-	-	-	-	-	-
Surface concentration (µm²/cm³) per alveolar fraction*							
AeroTrak 9000		[74-84.43]	[81.10-84.79]	[1.00-1.10]	52.88	53.37	1.01
Mass concentration (mg/m³)*							
DustTrak DRX	PM_1	-	-	-	-	-	-
	$PM_{2.5}$	-	-	-	-	-	-
	PM_{resp}	[40-123]	[53-471]	[1.04-3.84]	65	66	1.02
	PM_{10}	-	-	-	-	-	-
	PM_{total}	-	-	-	-	-	-

BG: background concentration; T: measurement taken while task performed; R: ratio of T to BG

*Concentrations reported as geometric means.

[1]Mean concentration intervals are reported when several measurements were taken for the same task: in this case, two measurements were systematically taken with each instrument for activities 3 and 4, and the DustTrak DRX was also used for activity 4.

Table 10 – Mean number, mass and surface (per alveolar fraction) concentrations measured with DRIs during different tasks performed by workers at site S2

S2 – 1 to 2		Activity 1			Activity 2		
Instrument		**BG**	**T**	**R**	**BG**	**T**	**R**
Number concentration (particles/cm³)							
P-Trak		2,400	3,100	1.29	1,500	1,400	0.93
AeroTrak 9306	0.3 µm	126	135	1.07	12.8	13.4	1.05
	0.5 µm	20.6	23.3	1.13	1.8	4.5	2.50
	1 µm	4.2	5.9	1.40	0.3	3.6	12.0
	3 µm	0.42	0.63	1.50	0.03	0.8	26.7
	5 µm	0.4	0.61	1.53	0.04	1.3	32.5
	10 µm	0.07	0.11	1.57	0.01	0.5	50.0
Surface concentration (µm²/cm³) per alveolar fraction							
AeroTrak 9000		33.3	35.57	1.07	43.14	42.49	0.98
Mass concentration (mg/m³)							
DustTrak DRX	PM_1	0.047	0.089	1.89	0.0045	0.185	41.1
	$PM_{2,5}$	0.048	0.09	1.88	0.0045	0.195	43.3
	PM_{resp}	0.049	0.092	1.88	0.0046	0.223	48.5
	PM_{10}	0.053	0.097	1.83	0.0048	0.451	94.0
	PM_{total}	0.053	0.097	1.83	0.006	0.604	101

Table 11 – Mean number, mass and surface (per alveolar fraction) concentrations measured with DRIs during different tasks performed by workers at site S3

S3 – 1 to 3		Activity 1			Activity 2			Activity 3		
Instrument		**BG**	**T**	**R**	**BG**	**T**	**R**	**BG**	**T**	**R**
Number concentration (particles/cm³)										
P-Trak		2,213	2,350	1.06	2,213	2,420	1.09	2,213	3,580	1.62
AeroTrak 9306	0.3 µm	49.1	53.1	1.08	49.1	59.8	1.22	49.1	50.8	1.03
	0.5 µm	8	8.8	1.10	8	10.3	1.29	8	10	1.25
	1 µm	0.7	0.8	1.14	0.7	1.03	1.47	0.7	1.4	2.00
	3 µm	0.03	0.04	1.33	0.03	0.07	2.33	0.03	0.09	3.00
	5 µm	0.02	0.03	1.50	0.02	0.08	4.00	0.02	0.1	5.00
	10 µm	0.004	0.005	1.25	0.004	0.02	5.00	0.004	0.03	7.50
Surface concentration (µm²/cm³) per alveolar fraction										
AeroTrak 9000		0.4	0.4	1.00	0.4	6	15.0	0.4	15	37.5
Mass concentration (mg/m³)										
DustTrak DRX	PM_1	-	-	-	-	-	-	-	-	-
	$PM_{2,5}$	-	-	-	-	-	-	-	-	-
	PM_{resp}	-	-	-	-	-	-	-	-	-
	PM_{10}	-	-	-	-	-	-	-	-	-
	PM_{total}	23	29	1.26	23	110	4.78	23	1090	47.4

S3 – 4 to 5		Activity 4			Activity 5		
Instrument		**BG**	**T**	**R**	**BG**	**T**	**R**
Number concentration (particles/cm³)							
P-Trak		20,240	28,045	1.39	29,860	19,890	0.67
AeroTrak 9306	0.3 µm	113.4	102	0.90	58.8	80	1.36
	0.5 µm	19.9	31.3	1.57	8.8	13.2	1.50
	1 µm	1.7	5.5	3.24	0.9	1	1.11
	3 µm	0.1	0.2	2.00	0.06	0.08	1.33
	5 µm	0.1	0.1	1.00	0.05	0.08	1.60
	10 µm	0.02	0.01	0.50	0.01	0.01	1.00
Surface concentration (µm²/cm³) per alveolar fraction							
AeroTrak 9000		72	82	1.14	70	49	0.70
Mass concentration (mg/m³)							
DustTrak DRX	PM_1	-	-	-	-	-	-
	$PM_{2.5}$	-	-	-	-	-	-
	PM_{resp}	-	-	-	-	-	-
	PM_{10}	-	-	-	-	-	-
	PM_{total}	50	60	1.20	38	33	0.87

Table 12 – Mean number, mass and surface (per alveolar fraction) concentrations measured with DRIs during different tasks performed by workers at site S4 with two different materials (A and B)

S4 – 1 to 3 (A)		Activity 1			Activity 2			Activity 3		
Instrument		**BG**	**T**	**R**	**BG**	**T**	**R**	**BG**	**T**	**R**
Number concentration (particles/cm³)										
P-Trak		1,600	1,500	0.94	1,600	1,600	1.00	1,900	2,000	1.05
AeroTrak 9306	0.3 µm	61	57	0.93	41	38	0.93	26	35	1.35
	0.5 µm	7	7	1.00	5	5	1.00	5	8	1.60
	1 µm	0.2	0	0.00	0.3	1	3.33	2	4	2.00
	3 µm	0.006	0.015	2.50	0.03	0.1	3.33	0.3	0.7	2.33
	5 µm	0	0.01	NA	0.03	0.1	3.33	0.2	0.6	3.00
	10 µm	0	0	NA	0	0.02	NA	0	0.1	NA
Surface concentration (µm²/cm³) per alveolar fraction										
AeroTrak 9000		18	18	1.00	16	15	0.94	10	13	1.30
Mass concentration (mg/m³)										
DustTrak DRX	PM_1	0.02	0.02	1.00	0.01	0.02	2.00	0.01	0.04	4.00
	$PM_{2.5}$	0.02	0.02	1.00	0.01	0.02	2.00	0.01	0.04	4.00
	PM_{resp}	0.02	0.02	1.00	0.01	0.02	2.00	0.01	0.05	5.00
	PM_{10}	0.02	0.02	1.00	0.01	0.02	2.00	0.01	0.05	5.00
	PM_{total}	0.02	0.02	1.00	0.01	0.02	2.00	0.02	0.05	2.50

S4 – 1 to 3 (B)		Activity 1			Activity 2			Activity 3		
Instrument		**BG**	**T**	**R**	**BG**	**T**	**R**	**BG**	**T**	**R**
Number concentration (particles/cm³)										
P-Trak		2,300	2,400	1.04	1,500	1,700	1.13	1,300	1,300	1.00
AeroTrak 9306	0.3 µm	72	78	1.08	15	29	1.93	37	36	0.97
	0.5 µm	9	1	0.11	2	6	3.00	4	12	3.00
	1 µm	0.4	0.4	1.00	0.2	6	30.0	0.4	11	27.5
	3 µm	0.03	0.03	1.00	0.02	1.8	90.0	0.05	1.9	38.0
	5 µm	0.02	0.02	1.00	0.02	1.9	95.0	0.05	1.4	28.0
	10 µm	0	0	NA	0	0.6	NA	0	0.3	NA
Surface concentration (µm²/cm³) per alveolar fraction										
AeroTrak 9000		15	17	1.13	10	11	1.10	8	11	1.38
Mass concentration (mg/m³)										
DustTrak DRX	PM_1	0.02	0.03	1.50	0.02	0.15	7.50	0.01	0.2	20.0
	$PM_{2.5}$	0.02	0.03	1.50	0.02	0.16	8.00	0.01	0.21	21.0
	PM_{resp}	0.02	0.03	1.50	0.02	0.18	9.00	0.01	0.23	23.0
	PM_{10}	0.02	0.03	1.50	0.02	0.3	15.0	0.01	0.29	29.0
	PM_{total}	0.02	0.03	1.50	0.02	0.32	16.0	0.01	0.29	29.0

Table 13 – Mean number, mass and surface (per alveolar fraction) concentrations measured with DRIs during different tasks performed by workers at site S5

S5		Activity 1		
Instrument		**BG**	**T**	**R**
Number concentration (particles/cm³)				
P-Trak		2,554	6,960	2.73
AeroTrak 9306	0.3 µm	448	306	0.68
	0.5 µm	59	70	1.19
	1 µm	2	46	23.0
	3 µm	0	6	NA
	5 µm	0	2	NA
	10 µm	0	0	NA
Surface concentration (µm²/cm³) per alveolar fraction				
AeroTrak 9000		-	-	-
Mass concentration (mg/m³)				
DustTrak DRX	PM_1	0.0445	0.104	2.34
	$PM_{2.5}$	0.0447	0.113	2.53
	PM_{resp}	0.0451	0.133	2.95
	PM_{10}	0.0467	0.158	3.38
	PM_{total}	0.0489	0.163	3.33

Table 14 – Mean number, mass and surface (per alveolar fraction) concentrations measured with DRIs during different tasks performed by workers at site S6

S6 – 1 to 4		Activity 1			Activity 2			Activity 3			Activity 4		
Instrument		**BG**	**T**	**R**	**BG**	**T**	**R**	**BG**	**T**	**R**	**BG**	**T**	**R**
Number concentration (particles/cm³)													
P-Trak		4,600	4,705	1.02	6,231	6,722	1.08	6,522	33,390	5.12	4,673	6,641	1.42
AeroTrak 9306	0.3 µm	7.5	8.2	1.09	12.2	12.4	1.02	6.1	5.6	0.92	4.8	9.2	1.92
	0.5 µm	1.2	1.3	1.08	2.2	2.2	1.00	1	0.9	0.90	0.8	1.7	2.13
	1 µm	0.04	0.05	1.25	0.1	0.1	1.00	0.04	0.04	1.00	0.04	0.07	1.75
	3 µm	0.001	0.0001	0.10	0.003	0.004	1.33	0.002	0.002	1.00	0.001	0.003	3.00
	5 µm	0.0008	0.00006	0.08	0.001	0.002	2.00	0.0008	0.0008	1.00	0.0009	0.001	1.11
	10 µm	0.0001	0.0001	1.00	0.0003	0.0002	0.67	0.001	0.0001	0.10	0.0002	0.0001	0.50
Surface concentration (µm²/cm³) per alveolar fraction													
AeroTrak 9000		33	40	1.21	68	68	1.00	36	99	2.75	29	54	1.86
Mass concentration (mg/m³)													
DustTrak DRX	PM_1	0.09	0.1	1.11	0.2	0.2	1.00	0.07	0.06	0.86	0.11	0.08	0.73
	$PM_{2.5}$	0.09	0.1	1.11	0.2	0.2	1.00	0.07	0.06	0.86	0.11	0.08	0.73
	PM_{resp}	0.09	0.1	1.11	0.2	0.2	1.00	0.07	0.06	0.86	0.11	0.08	0.73
	PM_{10}	0.13	0.1	0.77	0.2	0.2	1.00	0.07	0.06	0.86	0.11	0.08	0.73
	PM_{total}	0.13	0.1	0.77	0.2	0.2	1.00	0.07	0.06	0.86	0.11	0.08	0.73

S6 – 5 to 7		Activity 5			Activity 6			Activity 7		
Instrument		**BG**	**T**	**R**	**BG**	**T**	**R**	**BG**	**T**	**R**
Number concentration (particles/cm³)										
P-Trak		5,807	20,613	3.55	5,807	30,647	5.28	6,049	22,860	3.78
AeroTrak 9306	0.3 µm	7.9	8.9	1.13	8.7	9	1.03	4.6	5.8	1.26
	0.5 µm	1.1	1.4	1.27	1.4	1.4	1.00	0.7	0.8	1.14
	1 µm	0.03	0.1	3.33	0.1	0.1	1.00	0.04	0	0.00
	3 µm	0.003	0.01	3.33	0.01	0.02	2.00	0.002	0.001	0.50
	5 µm	0.004	0.007	1.75	0.009	0.03	3.33	0.001	0.0009	0.90
	10 µm	0.002	0.002	1.00	0.003	0.01	3.33	0.0003	0.0002	0.67
Surface concentration (µm²/cm³) per alveolar fraction										
AeroTrak 9000		42	72	1.71	58	118	2.03	41	173	4.22
Mass concentration (mg/m³)										
DustTrak DRX	PM_1	0.09	0.14	1.56	0.12	0.27	2.25	0.06	0.07	1.17
	$PM_{2.5}$	0.09	0.15	1.67	0.12	0.28	2.33	0.06	0.07	1.17
	PM_{resp}	0.09	0.15	1.67	0.12	0.29	2.42	0.06	0.07	1.17
	PM_{10}	0.09	0.17	1.89	0.13	0.48	3.69	0.07	0.07	1.00
	PM_{total}	0.1	0.17	1.70	0.13	0.48	3.69	0.07	0.07	1.00

Table 15 – Mean number, mass and surface (per alveolar fraction) concentrations measured with DRIs during different tasks performed by workers at site S7

S7 – 1 to 4		Activity 1			Activity 2		
Instrument		BG	T	R	BG	T	R
Number concentration (particles/cm³)							
P-Trak		2,143	23,867	11.14	2,143	4,107	1.92
AeroTrak 9306	0.3 µm	78,088	133,818	1.71	78,088	135,954	1.74
	0.5 µm	4,741	38,895	8.20	4,741	9,167	1.93
	1 µm	1,513	30,581	20.21	1,513	1,663	1.10
	3 µm	292	7,363	25.22	292	177	0.61
	5 µm	223	6,955	31.19	223	124	0.56
	10 µm	52	1,950	37.50	52	30	0.58
Surface concentration (µm²/cm³) per alveolar fraction							
AeroTrak 9000		5.2	31.1	5.98	5.2	8	1.54
Mass concentration (mg/m³)							
DustTrak DRX	PM_1	0.011	0.27	24.6	0.011	0.019	1.73
	$PM_{2.5}$	0.011	0.271	24.6	0.011	0.019	1.73
	PM_{resp}	0.011	0.274	24.9	0.011	0.019	1.73
	PM_{10}	0.011	0.274	24.9	0.011	0.019	1.73
	PM_{total}	0.011	0.274	24.9	0.011	0.019	1.73

S7 – 1 to 4		Activity 3			Activity 4		
Instrument		BG	T	R	BG	T	R
Number concentration (particles/cm³)							
P-Trak		2,143	413,091	193	2143	3911	1.83
AeroTrak 9306	0.3 µm	78,088	191,330	2.45	78,088	128,009	1.64
	0.5 µm	4,741	105,107	22.2	4,741	13,199	2.78
	1 µm	1,513	105,705	69.9	1,513	3,066	2.03
	3 µm	292	27,850	95.4	292	189	0.65
	5 µm	223	30,199	135	223	95	0.43
	10 µm	52	10,989	211	52	14	0.27
Surface concentration (µm²/cm³) per alveolar fraction							
AeroTrak 9000		5.2	2,120.5	408	5.2	11.1	2.13
Mass concentration (mg/m³)							
DustTrak DRX	PM_1	0.011	1.694	154	0.011	0.015	1.36
	$PM_{2.5}$	0.011	1.698	154	0.011	0.015	1.36
	PM_{resp}	0.011	1.709	155	0.011	0.016	1.45
	PM_{10}	0.011	1.713	156	0.011	0.016	1.45
	PM_{total}	0.011	1.713	156	0.011	0.016	1.45

Table 16 – Mean number, mass and surface (per alveolar fraction) concentrations measured with DRIs during different tasks performed by workers at site S8

S8		**Activity 1**		
Instrument		**BG**	**T**	**R**
Number concentration (particles/cm³)				
P-Trak		3,400	18,796	5.53
AeroTrak 9306	0.3 µm	-	-	-
	0.5 µm	-	-	-
	1 µm	-	-	-
	3 µm	-	-	-
	5 µm	-	-	-
	10 µm	-	-	-
Surface concentration (µm²/cm³) per alveolar fraction				
AeroTrak 9000		20.5	88.1	4.30
Mass concentration (mg/m³)				
DustTrak DRX	PM_1	-	-	-
	$PM_{2.5}$	-	-	-
	PM_{resp}	-	-	-
	PM_{10}	-	-	-
	PM_{total}	0.0264	0.0605	2.29

Table 17 – Mean number, mass and surface (per alveolar fraction) concentrations measured with DRIs during different tasks performed by workers at site S9

S9 – 1 to 3		Activity 1			Activity 2			Activity 3		
Instrument		**BG**	**T**	**R**	**BG**	**T**	**R**	**BG**	**T**	**R**
Number concentration (particles/cm³)										
P-Trak		20,743	19,412	0.94	22,284	22,833	1.02	22,245	25,547	1.15
AeroTrak 9306	0.3 µm	12.7	15.6	1.23	12.4	10.9	0.88	12.5	14.6	1.17
	0.5 µm	2.49	3.4	1.37	2.8	2.6	0.93	3.1	3.8	1.23
	1 µm	0.2	0.2	1.00	0.2	0.2	1.00	0.02	0.3	15.0
	3 µm	0.01	0.01	1.00	0.01	0.02	2.00	0.01	0.02	2.00
	5 µm	0.008	1	NA	0.01	0.02	2.00	0.01	0.01	1.00
	10 µm	0.002	0.002	1.00	0.001	0.01	10.0	0.002	0.002	1.00
Surface concentration (µm²/cm³) per alveolar fraction										
AeroTrak 9000		96	118	1.23	106	139	1.31	134	141	1.05
Mass concentration (mg/m³)										
DustTrak DRX	PM_1	0.18	0.25	1.39	0.19	0.88	4.63	0.2	0.22	1.10
	$PM_{2.5}$	0.18	0.25	1.39	0.19	0.91	4.79	0.2	0.22	1.10
	PM_{resp}	0.18	0.25	1.39	0.19	0.95	5.00	0.2	0.22	1.10
	PM_{10}	0.18	0.25	1.39	0.19	0.99	5.21	0.2	0.22	1.10
	PM_{total}	0.18	0.25	1.39	0.19	0.99	5.21	0.2	0.22	1.10

S9 – 4 to 6		Activity 4			Activity 5			Activity 6		
Instrument		**BG**	**T**	**R**	**BG**	**T**	**R**	**BG**	**T**	**R**
Number concentration (particles/cm³)										
P-Trak		27,616	25,544	0.92	21,638	28,239	1.31	22,245	28,140	1.27
AeroTrak 9306	0.3 µm	15.4	15.8	1.03	8.8	13.1	1.49	14.2	11.6	0.82
	0.5 µm	2.5	3.2	1.28	2.2	3.3	1.50	3.1	2.7	0.87
	1 µm	0.1	0.4	4.00	0.2	0.3	1.50	0.13	0.24	1.85
	3 µm	0.003	0.07	23.3	0.01	0.01	1.00	0.01	0.03	3.00
	5 µm	0.002	0.08	40.0	0.01	0.01	1.00	0.002	0.03	15.0
	10 µm	0.001	0.03	30.0	0.002	0.004	2.00	0.001	0.01	10.0
Surface concentration (µm²/cm³) per alveolar fraction										
AeroTrak 9000		133	133	1.00	90	145	1.61	232	293	1.26
Mass concentration (mg/m³)										
DustTrak DRX	PM_1	0.26	0.8	3.08	0.13	0.23	1.77	0.3	5.11	17.0
	$PM_{2.5}$	0.26	0.91	3.50	0.13	0.23	1.77	0.3	5.21	17.4
	PM_{resp}	0.26	0.95	3.65	0.13	0.24	1.85	0.3	5.3	17.7
	PM_{10}	0.26	1.02	3.92	0.13	0.24	1.85	0.3	5.35	17.8
	PM_{total}	0.27	1.02	3.78	0.13	0.24	1.85	0.3	5.35	17.8

5.2.1.2 Particle size distributions (DRIs)

Particle-size distributions estimated using EEPSs and ELPIs were significantly different depending on the study site. While the ELPIs systematically showed particulate emissions, the EEPSs were much less useful, except at site S5. During activities at sites S1 and S3, for example, as the plots in Figure 13 and Figure 14 show, there was an increase in particles ranging in diameter from several hundred nanometres to several micrometres. Figure 15, on the other hand, which illustrates the situation at site S5, shows generation of particles that are mainly smaller than 100 nm.

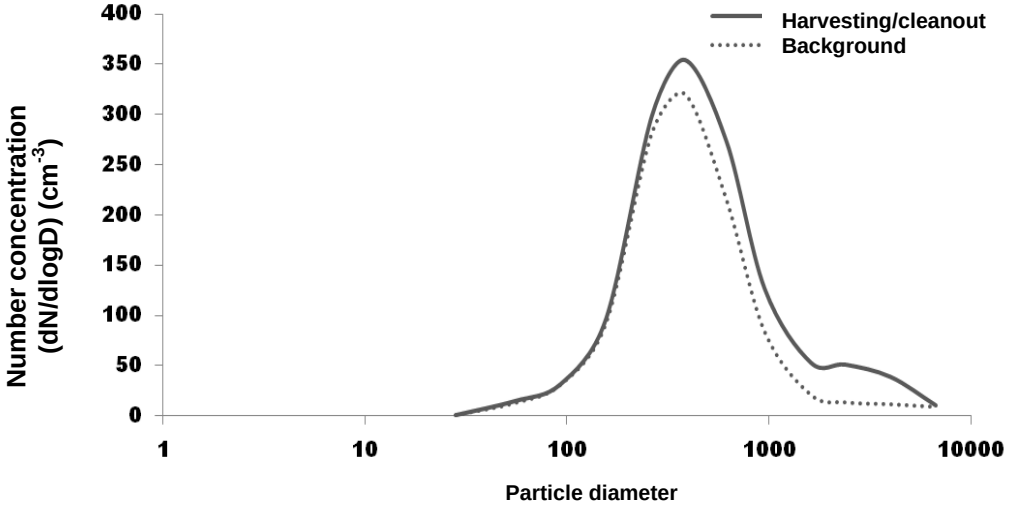

Figure 13 – Size distribution of particles generated during activity 4 (harvesting and cleanout) at site S1.

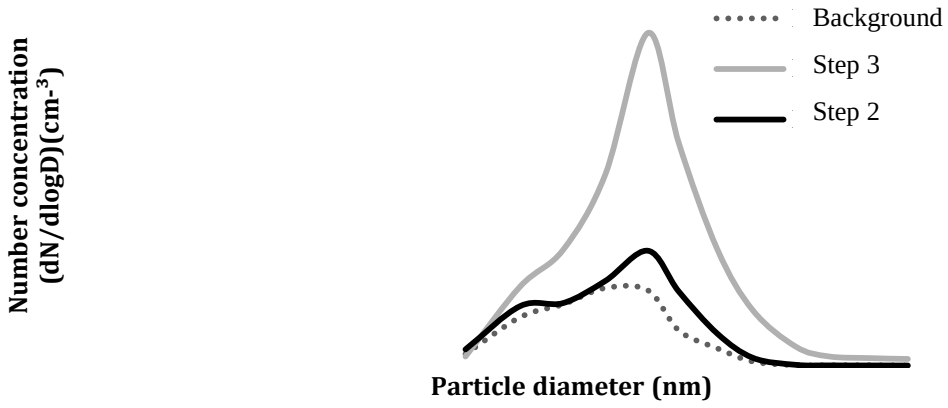

Figure 14 – Size distribution of particles generated during activities 2 and 3 of the process implemented at site S3.

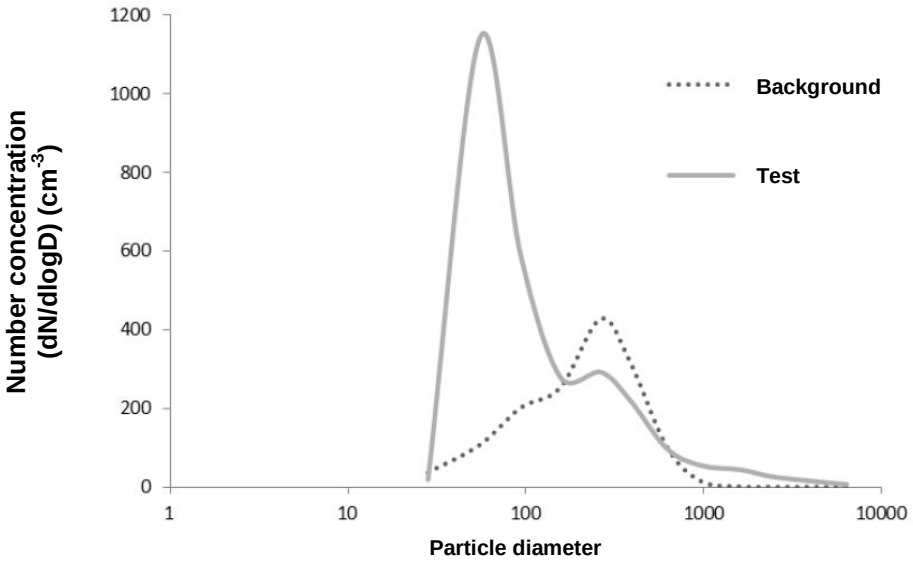

Figure 15 – Size distribution of particles generated during activity 1 (ink flow test) investigated at site S5

5.2.1.3 SEM/TEM analysis results

5.2.1.3.1 Use of grids on filters (37-mm cassettes) (sites S1 to S9)

Figures 16 to 27 show SEM and TEM images of particles collected on microscopy grids glued to a PTFE filter and placed in a 37-mm cassette. The figures show presence of the following: i) fibrous particles at sites S1, S4 and S6; ii) spherical particulate units of nanometric size at sites S3, S5 and S8; and iii) micrometric particles of no particular shape at sites S2, S7 and S9.

Site S1. Figure 16 shows SEM images of samples collected at site S1. Present are CNT agglomerates and highly agglomerated spherical carbon particles identified as carbon black particles. Round elements identified as the catalysts used in production are incorporated in the CNTs, as shown in Figure 17, which shows the results of the TEM-EDS analysis. Note as well the peaks of carbon (C), oxygen (O) and copper (Cu) found in all the spectra, as these are components associated with the microscopy grid. Note as well the peaks of iron (Fe) and nickel (Ni), characteristic of the metals used as catalysts.

Site S2. The SEM images in Figure 18 are of particles collected during activity 2 (drying and bagging of nanocrystalline cellulose). Note the particles of micrometric size with rounded or amorphous shapes.

Site S3. Figure 19 shows SEM images of particles collected during activities 2 and 4 at site S3. The vast majority of the particles are spherical, isolated or agglomerated and range in size from 10 to 1,000 nm.

Site S4. Figure 20 and Figure 21 show images of particles collected during activities at site S4. Note the presence of agglomerates with spherical as well as fibrous particles. TEM-EDS analysis indicates systematic presence of Ti, Fe and P in the analyses during the different stages of the process investigated (see Table 18). This confirms that the particles generated do indeed come from the powders used in the mechanofusion.

Site S5. Figure 22 shows SEM images of isolated or agglomerated particles collected at site S5. TEM image analysis (Figure 23) shows spherical bismuth (Bi) particles ranging in size from 100 to 200 nm and smaller rectangular, triangular and hexagonal zinc particles. TEM-EDS analysis indicates presence of Zn in 70% of the particles analyzed and presence of Bi in 25% of the particles analyzed, confirming that the particles generated do indeed come from the ink used for the tests at these sites.

Site S6. Figure 24 shows particles collected during activity 5 and activity 6 (sawing and sanding/polishing of nanocomposites) at site S6. Fibrous particles (possibly MWCNTs) trapped in a matrix, are visible in both images.

Site S7. Figure 25 shows isolated or agglomerated spherical or angular particles ranging in size from 100 nm to 2 μm. EDS analysis indicates presence of a number of elements, including silica (Si), sodium (Na), chlorine (Cl) and potassium (K), confirming that the particles generated do indeed come from the nanoclays used at site S7.

Site S8. Figure 26 shows TEM images of particles collected in the breathing zone of workers at site S8, during varnishing of wood floors containing NPs of TiO_2 and SiO_2. The vast majority of the TiO_2 agglomerates are spherical and composed of NPs of TiO_2 that individually measure 5 to 20 nm. The SiO_2 agglomerates are composed of spherical NPs about 20 nm to 200 nm in diameter. All the TiO_2 and SiO_2 agglomerates are covered with a film and can measure up to several micrometres. The film seems to indicate deposit on the grids in the form of fine droplets.

Site S9. Figure 27 shows SEM images of particles collected at site S9. There are no fibrous particles, but rather agglomerates of no particular shape. Chlorine (Cl), associated with the acids used during digestion and functionalization, is present in all spectra of the EDS analysis.

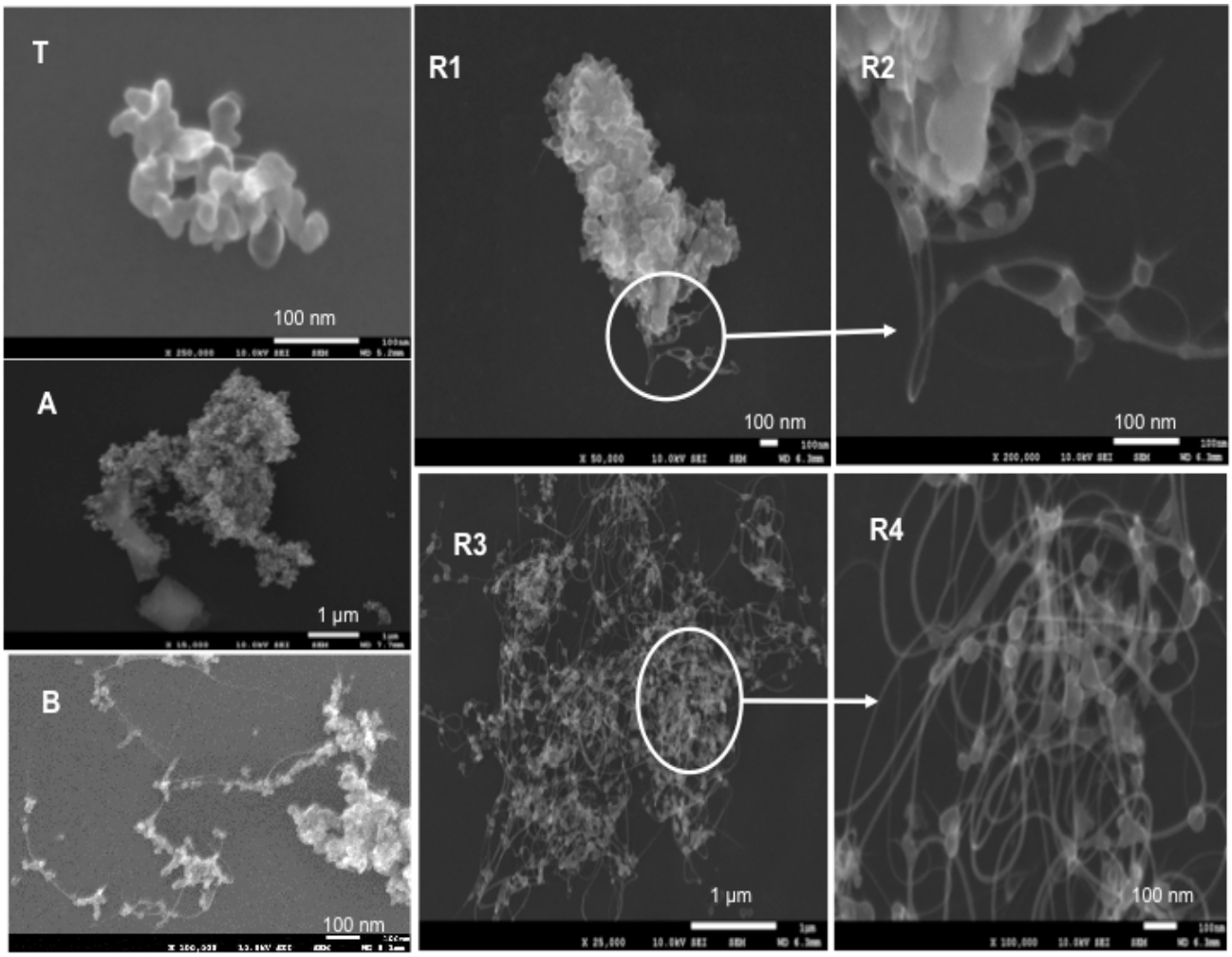

Figure 16 – SEM images of airborne particles collected during activities 3 (T) and 4 (R1 to R4) and of particles collected on surfaces in two different rooms (A and B) at site S1

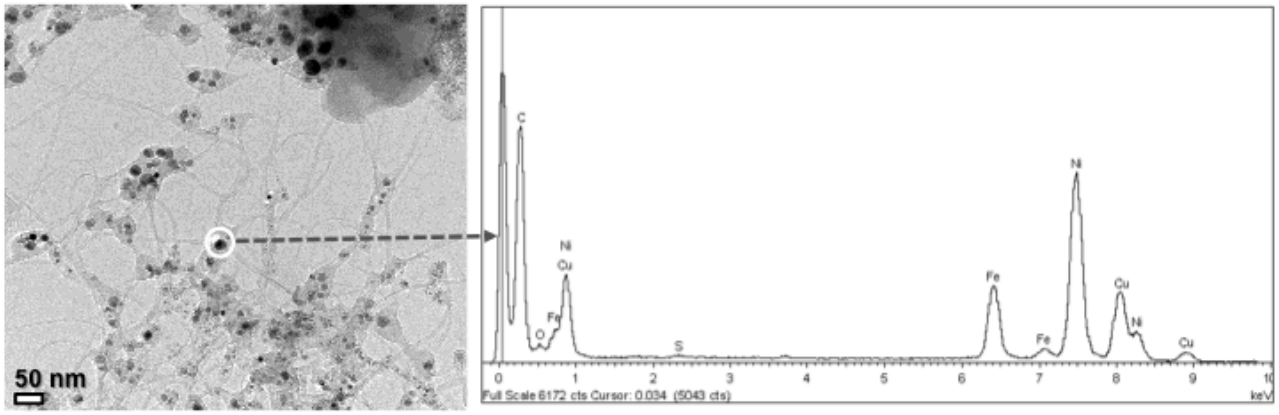

Figure 17 – TEM-EDS analysis of a sample collected at site S1 during activity 4

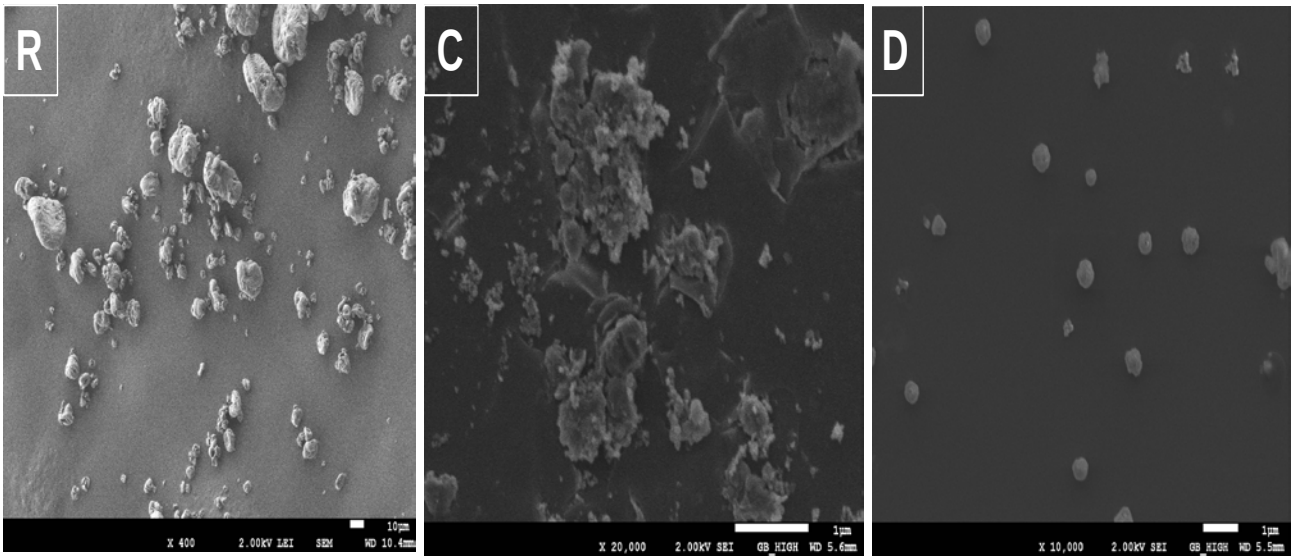

Figure 18 – SEM images of particles collected in air inhaled by workers at site S2 during activity 2 (R, C and D)

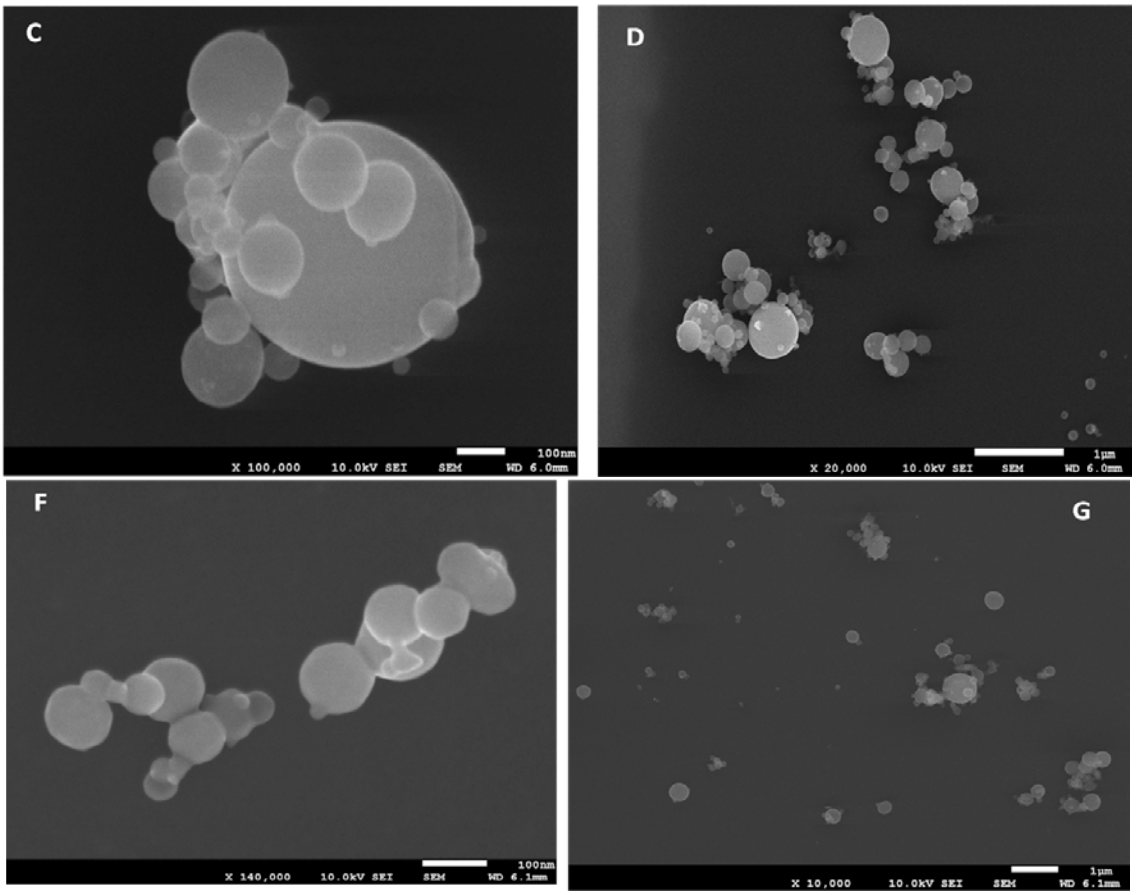

Figure 19 – SEM images of particles collected in workers' breathing zone at site S3 during activities 2 (C and D) and 4 (F and G)

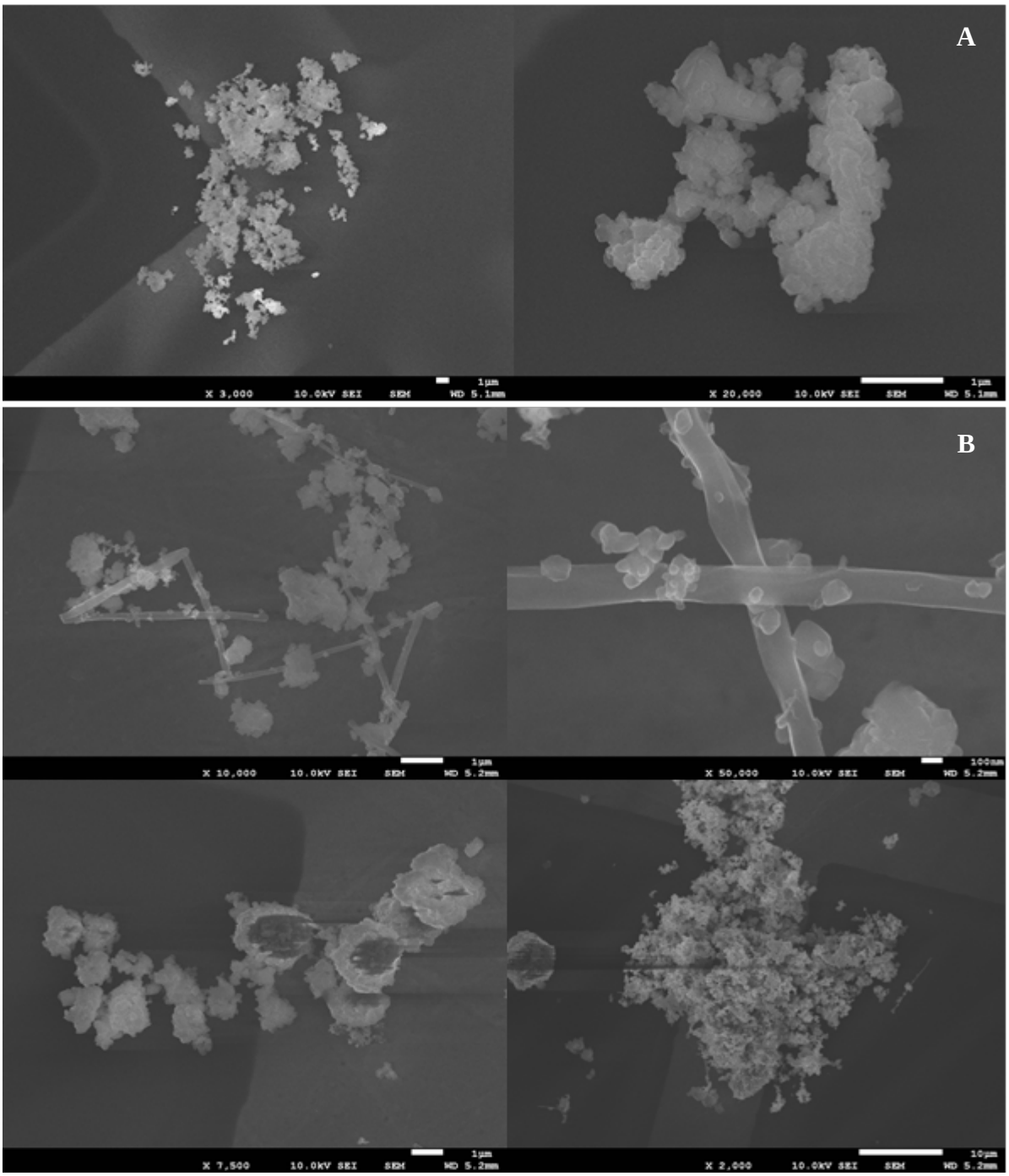

Figure 20 – SEM images of particles collected in workers' breathing zone at site S4 during activities 1 (A) and 2 (B)

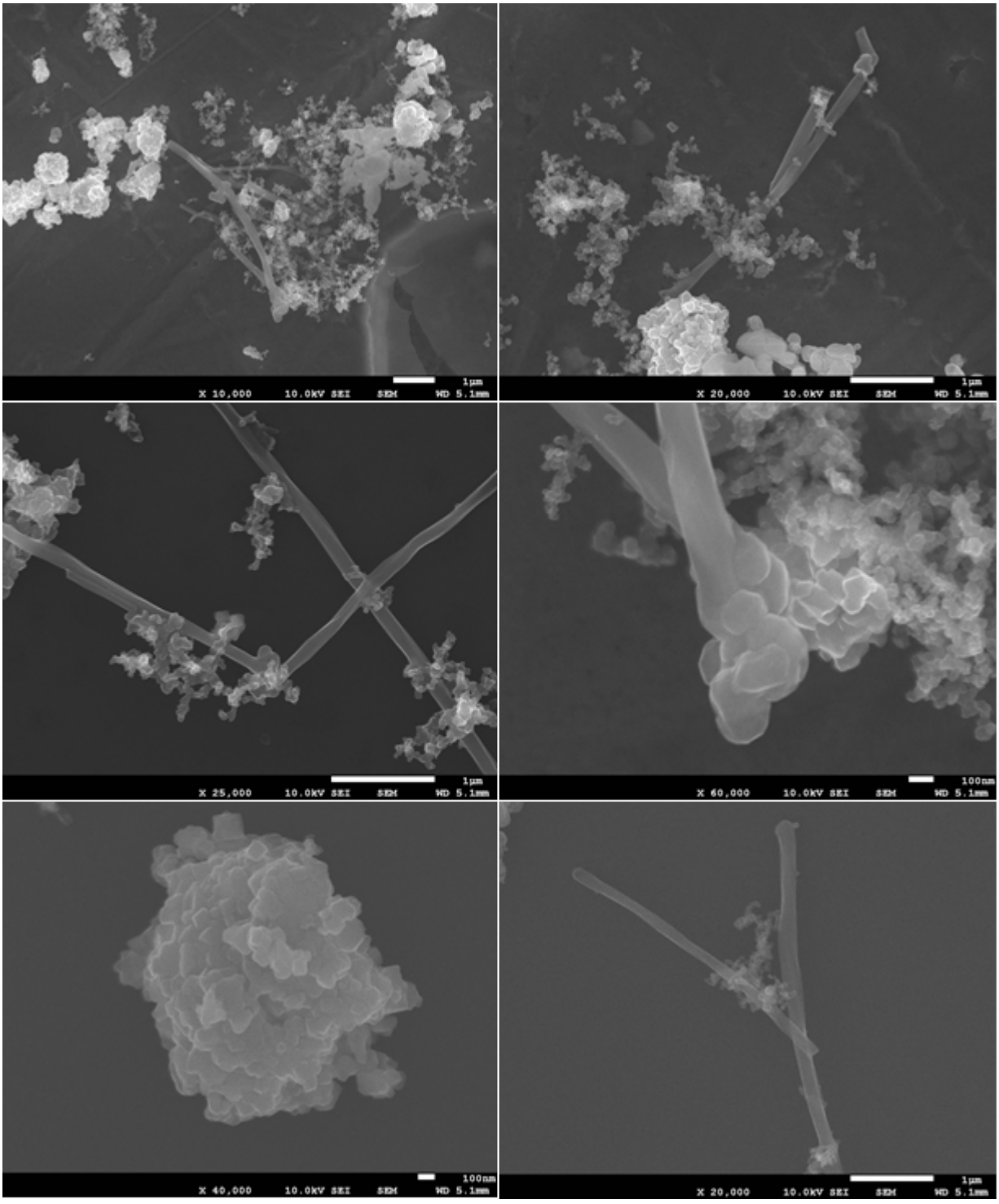

Figure 21 – SEM images of particles collected in workers' breathing zone at site S4 during activity 3

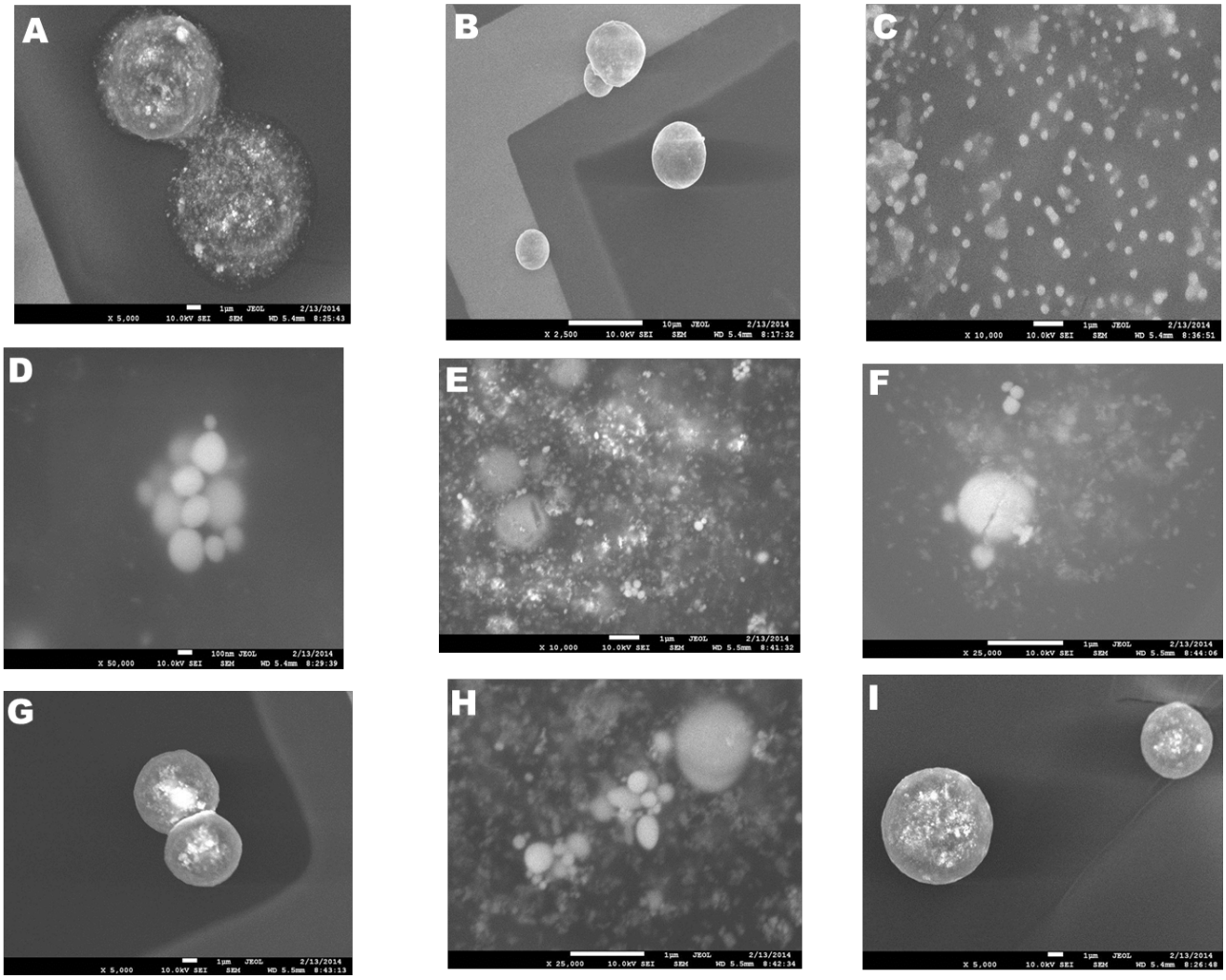

Figure 22 – SEM images of particles collected in workers' breathing zone at site S5

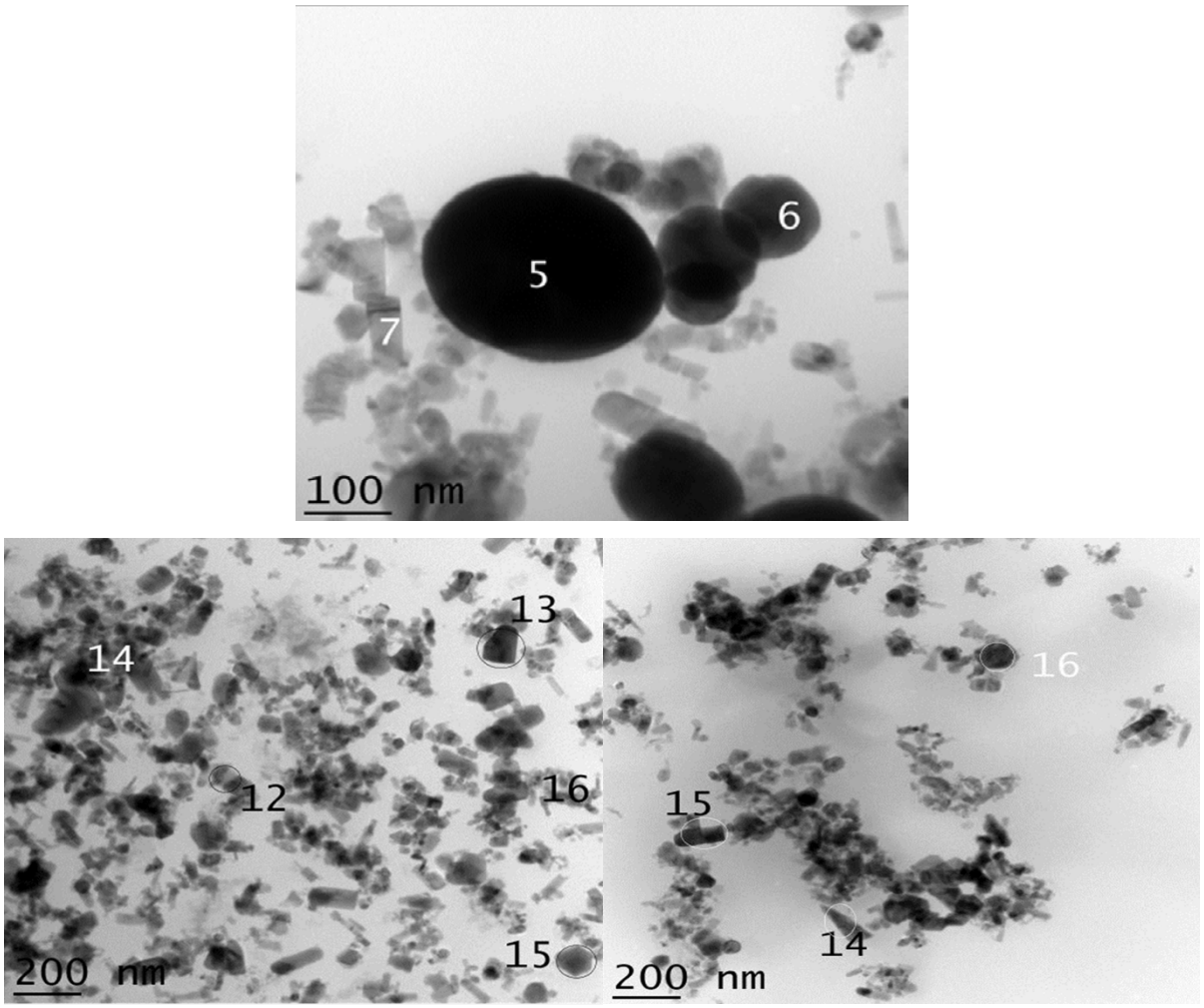

Figure 23 –TEM images of particles collected in workers' breathing zone at site S5

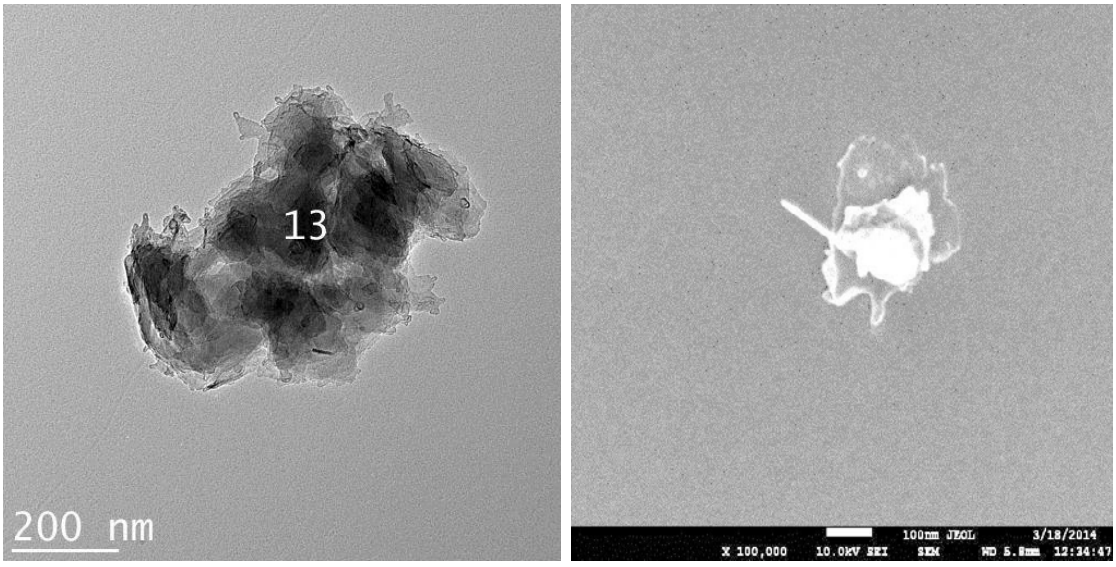

Figure 24 – TEM and SEM images of particles collected in workers' breathing zone at site S6 during activities 5 and 6

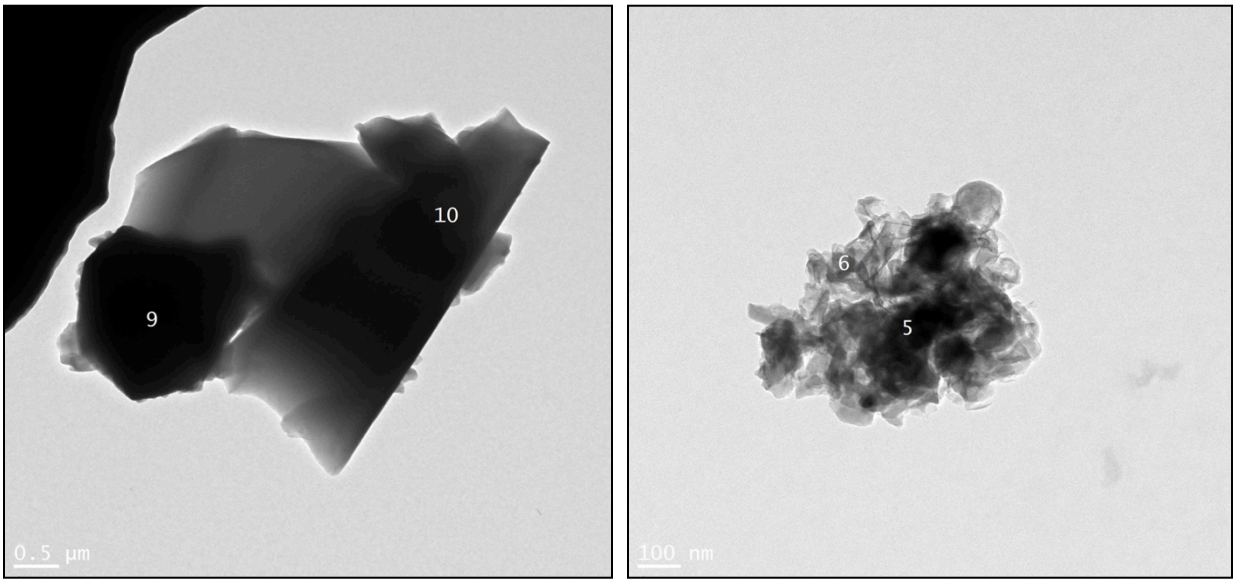

Figure 25 – TEM images of particles collected in workers' breathing zone at site S7 during activity 2

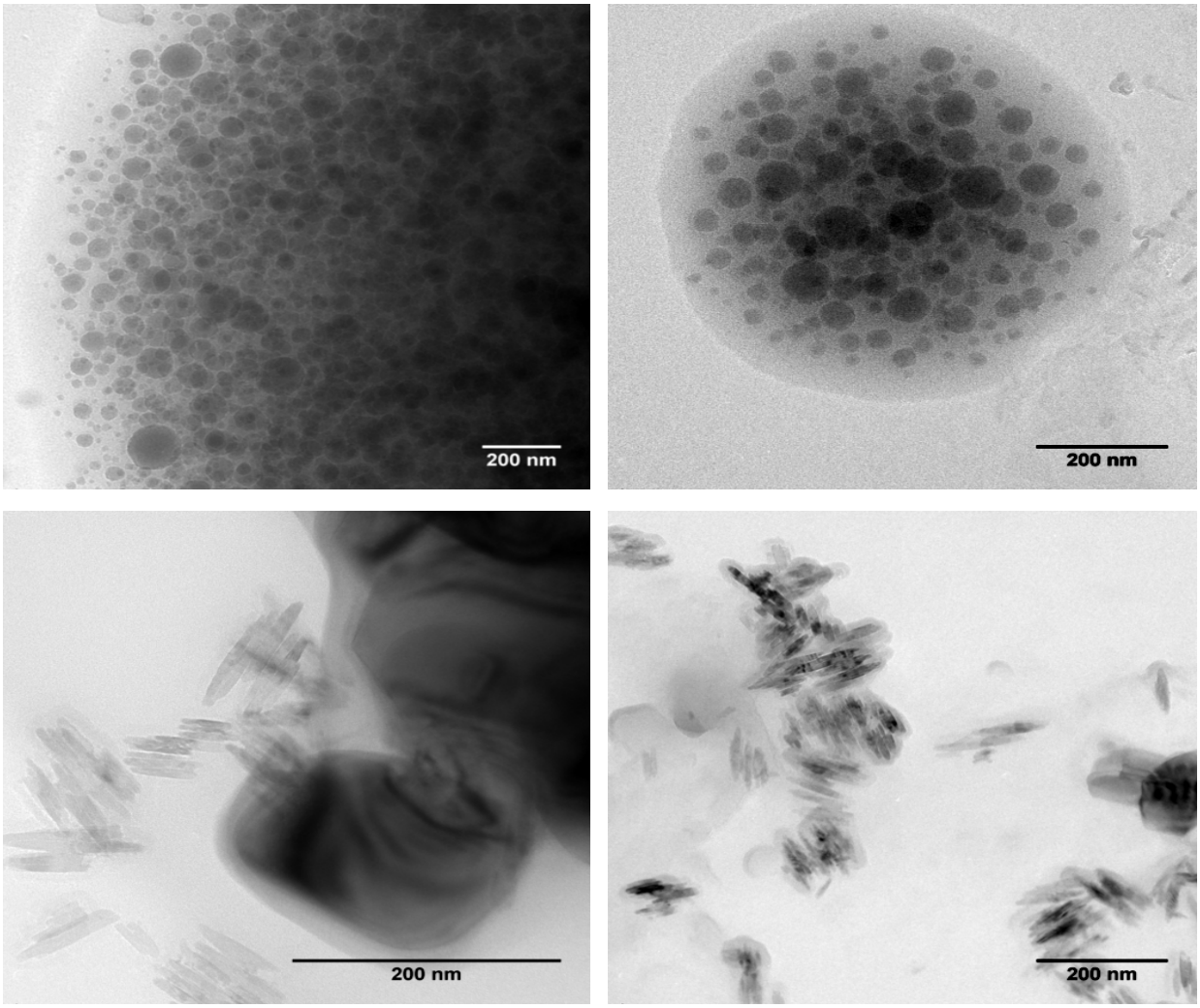

Figure 26 – TEM images of particles collected in workers' breathing zone at site S8 during varnishing

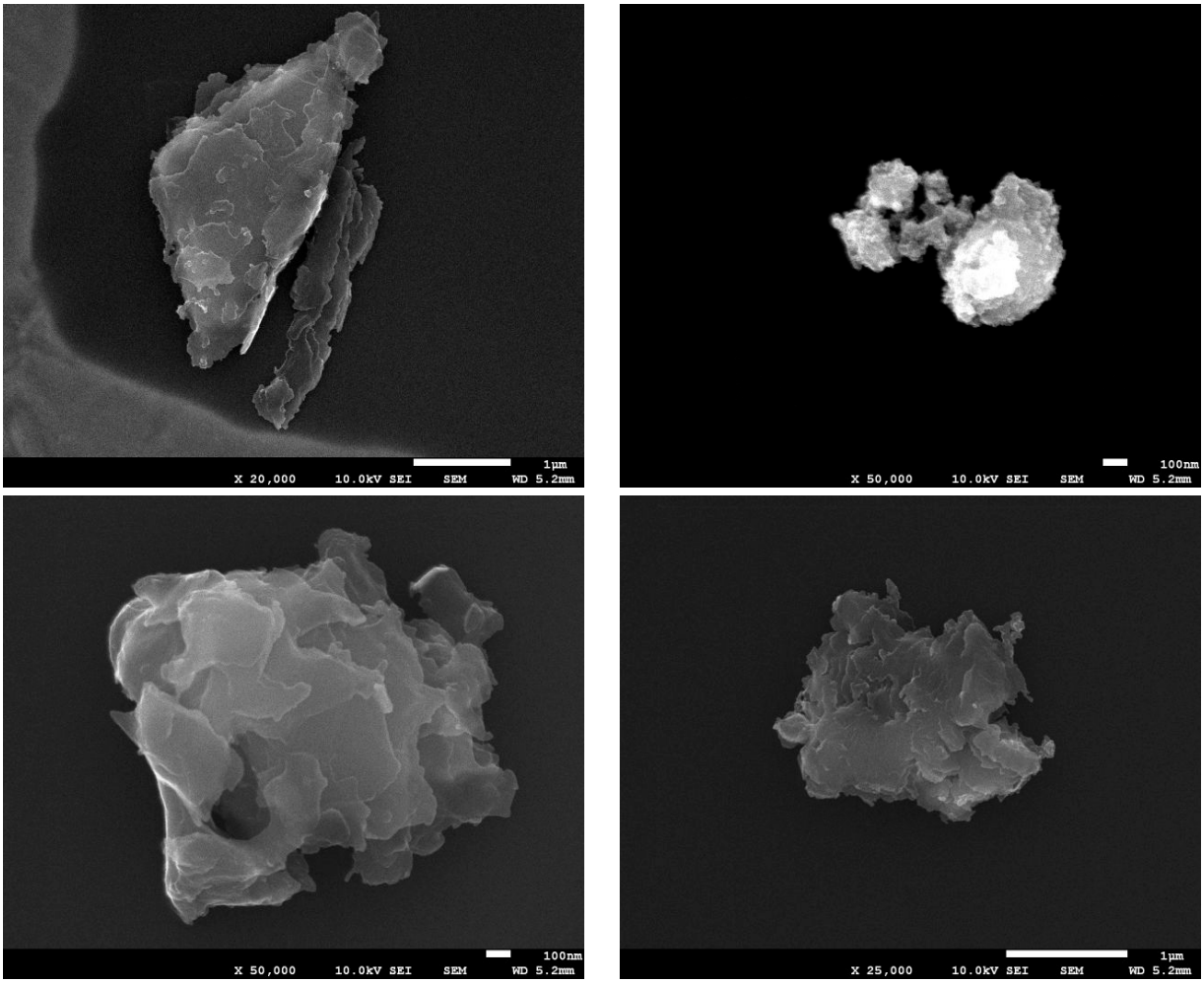

Figure 27 – SEM images of particles collected in workers' breathing zone at site S9 during activity 5

5.2.1.3.1.1 Results of TEM-EDS analyses

In addition to the morphological analyses discussed above, the elemental chemical composition of the particles collected was determined through identification of TEM-EDS spectrum. EDS spectrum peak identification made it possible to determine this composition. Table 18 lists the five main elements found at sites S1 through S9 in order of frequency.

Table 18 – Five elements most frequently identified by TEM-EDS on microscopy grids at each site

Site	S1	S2	S3	S4	S5	S6	S7	S8	S9
Elements identified by EDS	Fe Ni Co Cl S	S Fe Cl Cr Ni	Cu Si S Ca	Ti, Fe P Pb S	Zn Cl Fe Bi Al	-	Na P Si K Cl	Ti Si	Cl Fe Al K Mg

5.2.1.3.2 Use of the Mini Particle Sampler (MPS) (sites S1 and S8)

An MPS equipped with filtering index grids offers a direct method of sampling in the worker's breathing zone (see Section 2.2.1.3.3). Different analyses can then be performed to characterize exposure concentrations. The methods used for SWCNT calculation (site S1) and TiO_2 and SiO_2 determination (site S8) are described below.

5.2.1.3.2.1 Site S1

Particles that are fibrous or that contain fibres were counted in 15 microscopy grid squares, giving an average of 8.33 SWCNT structures per square (Table 19). Each grid square measures 48.6 µm by 52.5 µm (2,551.5 µm²). As the opening of the MPS does not cover the entire grid (Figure 28), the size of the opening surface through which the analyzed air passes was determined by image analysis to be 1,792,737 µm². A square is thus 0.14% of the grid opening. With flow at 0.3 L/min for 180 min, a sampling volume of 54 L was collected, that is, 0.077 L per square (assuming uniform air flow). Calculated concentration was thus 108 structures per litre of air, or 0.108 SWCNT/cm³.

Table 19 – CNT fibrous structure count per microscopy grid square and grid square identification (site S1)

Square	Number of structures noted
G-2+2	9
G-2+1	4
G-2-1	8
G-2-2	7
G-1-2	12
N-2+2	8
N-2+1	7
N-2-1	9
N-2-2	7
N+2+2	1
N+1+1	5
N+2-1	16
U-2+2	11
U-2+1	3
U-2-1	18

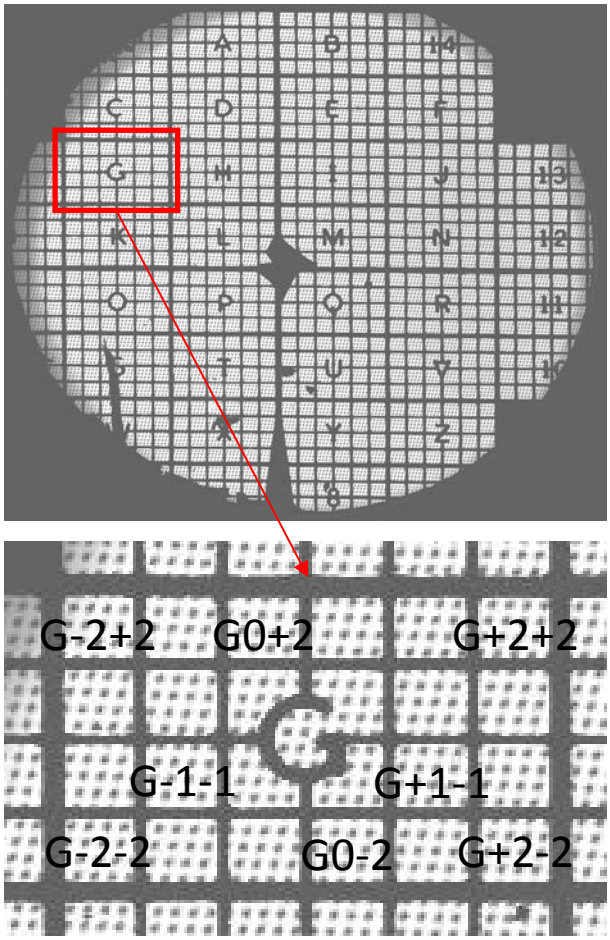

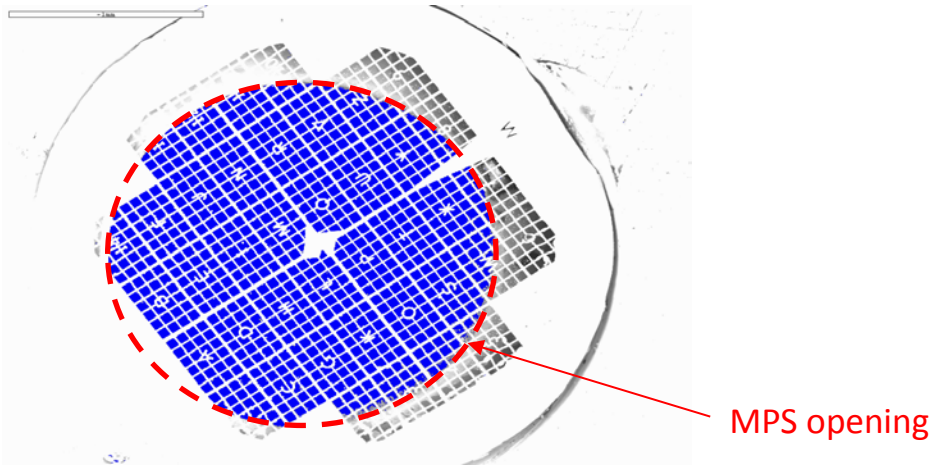

Figure 28 – Drawing of opening of microscopy grid used in an MPS as determined by image analysis (site S1)

5.2.1.3.2.2 Site S8

Parallel analyses were performed of samples collected with the MPS (filtering grid) and with a 37-mm cassette (solid grid) in the worker's breathing zone during varnishing. Table 20 shows estimated particle counts per grid opening. An average of 194 particles per opening was calculated with the MPS, compared to 3 particles per opening with the 37-mm cassette. The percentage of particles of TiO_2 and SiO_2 differed depending on the sampling technique used—with the majority of particles being SiO_2 (61%) with the MPS and the majority being TiO_2 (65%) with the 37-mm cassette.

Table 20 – Counts of particles collected on microscopy grids during finishing of wood floors with a varnish containing nanoparticles of TiO_2 and SiO_2 at site S8

Grid support	TiO_2		SiO_2		Number of openings analyzed	Number of particles per opening
	Particle count	%	Particle count	%		
MPS	151	39	236	61	2	194
Filter on cassette	98	65	52	35	50	3

5.2.1.4 Elemental carbon and gravimetric analyses (site S1)

Table 21 shows the results of analyses of elemental carbon and respirable dust from parallel sample collection for 30 to 40 minutes over four sampling days at site S1 during activity 4 (harvesting and cleanout). The respirable fraction concentrations measured ranged from below the detection limit to as much as 58 µg/m^3. Concentrations of the thoracic fraction ranged from 40 to 70 µg/m^3. The highest respirable dust concentration was 400 µg/m^3, and the lowest was below the detection limit of 25 µg.

Table 21 – Concentrations of elemental carbon (EC) and respirable dust measured in workers' breathing zone at site S1 during activity 4

	Concentration of EC (µg/m^3)			Concentration of respirable dust (µg/m^3)		
Test #	**Thoracic fraction PPI (2 L/min)**	**Respirable fraction PPI (8 L/min)**	**Respirable fraction GK2.69 (4.2 L/min)**	**DustTrak-DRX (GM)**	**37-mm cassette**	**37-mm cassette with grid**
#1	50	20	<9*	63	310	<120*
#2	40	<4*	-**	48	<103*	<102*
#3	70	58	<10*	73	<126*	<125*
#4	60	38	<11*	127	400	<138*

*: Not detected; GM: geometric mean

5.2.1.5 Raman spectroscopy (site S1)

In addition to the fibre counting described in Section 5.2.1.3.2.1, Raman spectroscopy analyses of the same microscopy grids were performed. Figure 29 shows reference spectra for the three wavelengths used (514 nm: 1st column; 633 nm: 2nd column and 785 nm: 3rd column) for the grids alone (first row), the grids plus carbon black (2nd row) and the grids plus SWCNTs (3rd row).

Calibration showed that the reference carbon black spectra were composed of two main peaks, at 1,350 cm^{-1} (D or defect band) and at 1,590 cm^{-1} (G or graphite band). These two peaks were found on the CNT reference spectra in addition to a peak at 2,600 cm^{-1} (G′ or 2D graphene band). Presence of this third peak thus signals the presence of CNTs in our samples. Wavelengths of 633 nm and 785 nm clearly demonstrate the presence of SWCNTs, unlike wavelengths of 514 nm.

Figure 30 shows 16 spectra observed on the microscopy grid used during sampling with the MPS at site S1. The grid regions analyzed were determined with an optical microscope. Note the peak at 2,600 cm^{-1} in regions #1, #3, #5 and #6, whereas all the other profiles appear similar to that of carbon black. By calibrating the G band of the SWCNT reference spectra at 100%, we estimated the amount of SWCNTs in the four samples presenting G′ peaks at 2.5 to 5.8%.

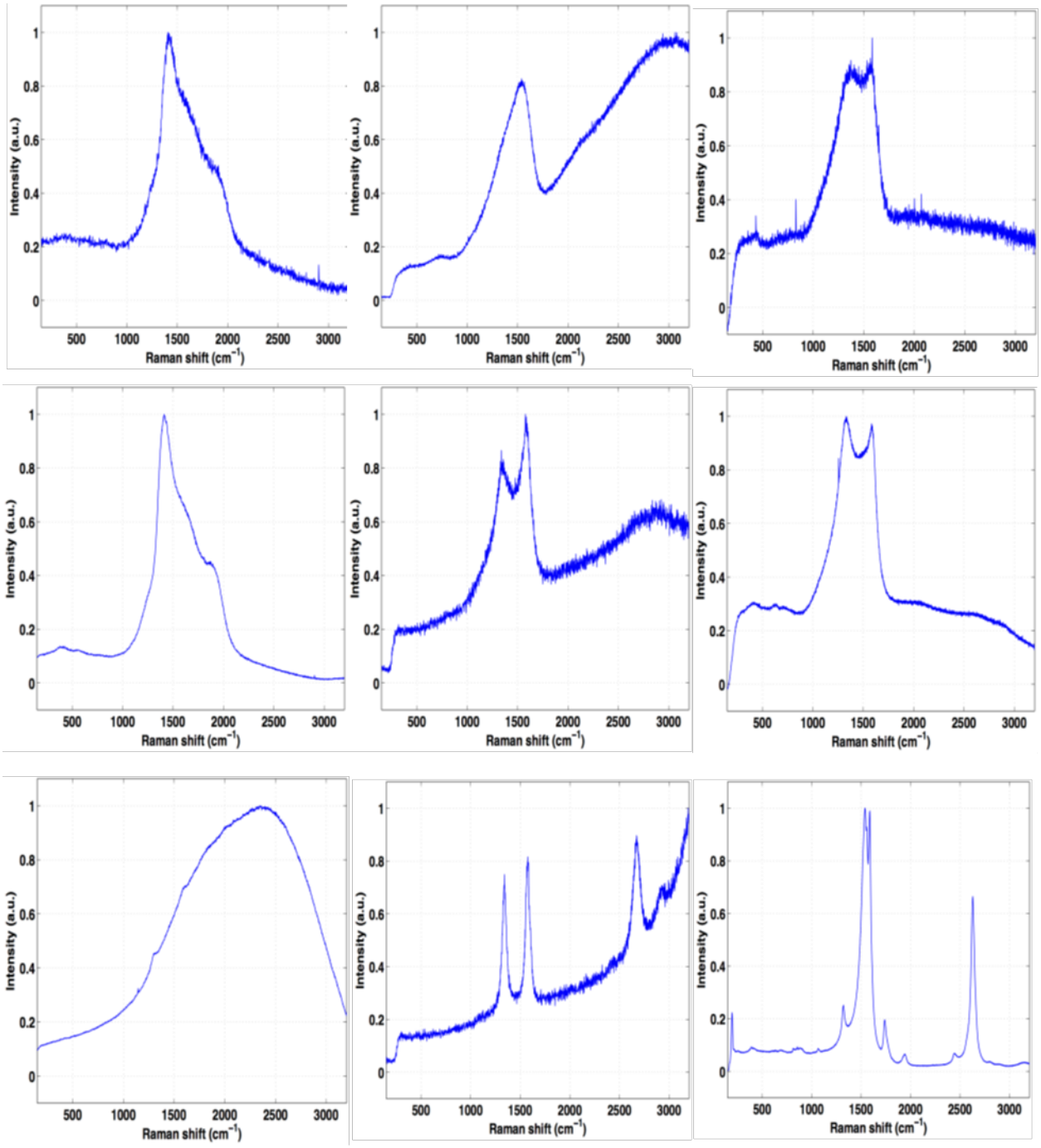

514 nm **633 nm** **785 nm**

Figure 29 – Reference spectra (wavelengths = 514, 633 and 785 nm) for grids alone (1st row), grids with carbon black (2nd row) and grids with SWCNT (3rd row) (site S1)

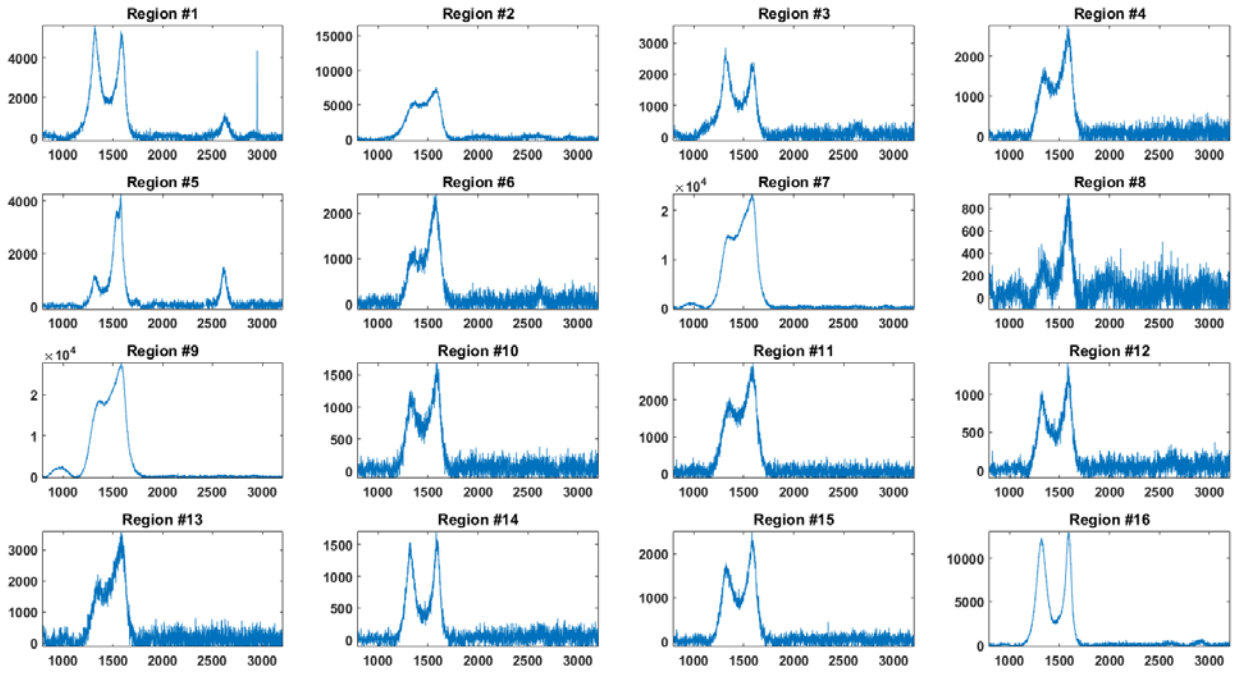

Figure 30 – Spectra of 16 microscopy grid analyses (site S1)

5.2.1.6 ICP-MS results (site S8)

Three personal measurements and one fixed-station measurement of TiO_2 concentrations were made using ICP-MS analyses of samples collected at site S8. The highest value recorded at the fixed station (as close as possible to the workstation investigated) was a TiO_2 concentration of 36 µg/m^3. The worker was exposed to 26 µg/m^3, whereas the two researchers observing him, slightly behind, were exposed to 11 µg/m^3.

5.2.2 Surface sampling

5.2.2.1 Site S1

Surfaces were sampled at three different locations in the workplace to assess the possibility of cross contamination. Measurements were taken in the production area below the reactor (two samples) and at a distance of 3 m from the reactor, in the change room, in the weighing room and in the conference room. CNT presence was confirmed only in the production hall (at two locations near the reactor). Metal elements (Fe and Co) associated with SWCNTs were also identified in these two samples (Table 22). Though presence of Fe was identified in all the samples, Co was only found close to the reactor.

Table 22 – Results of surface analyses at site 1

Sampling site	SWCNTs present	Carbon black present	Main chemical elements identified
Production hall (3 m from the reactor)	No	Yes	Ca, Al, Fe, S, Mg, P, Cl, Ti, K, Cr
Production hall (sample 1)	Yes	Yes	Fe, Co, Ni, Cl, S, Cl, Al, Ca, K, Mo
Production hall (sample 2)	Yes	Yes	Fe, Co, Ni, Cl, Al, K
Dispensing room	No	Yes	Cl, Fe, Ca, Al, S, K
Change room	No	Yes	S, Ca, Fe, Cl, Mg, Al, K, Ni, Cr
Conference room	No	No	Ca, Fe, Al; S, K, Mg, Ti, Cl, Cr, Ni

5.2.2.2 Site S4

Active sampling on a filter with a grid as well as sampling with a towelette was performed in the change rooms at site S4 before and after they were cleaned. The TEM image in Figure 31 shows a fibrous particle on a cluster of particles collected from the top of a door before cleaning. EDS analysis indicates presence of carbon on this fibre. A significant decrease (non-quantifiable) in the number of particles was noted in the microscopy analyses after cleaning. Only one of six surface samples showed presence of Ti before cleaning (Table 23).

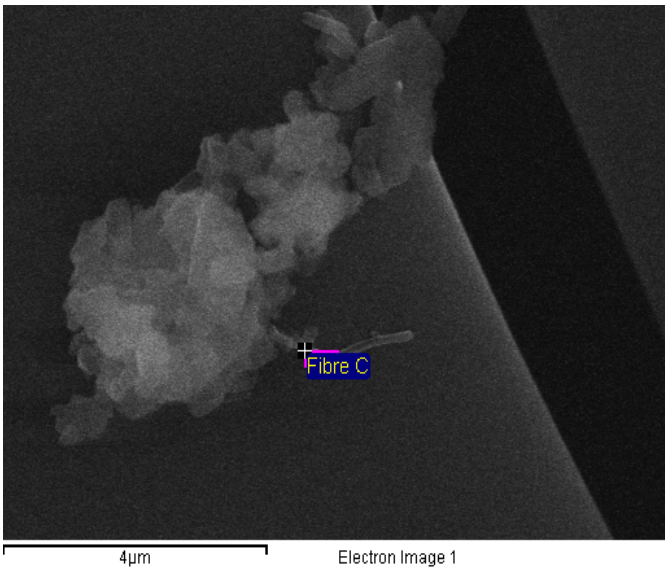

Figure 31– TEM image of fibrous particles collected at site S4.

Table 23 –Titanium measured on different surfaces before and after cleaning at site S4

Time of measurement	Site	Result	Time of measurement	Site	Result
Before cleaning	Locker near a laboratory door	0.5 µg	After cleaning	Near a laboratory door	<MRV
		<MRV			<MRV
		<MRV			<MRV
	Laboratory door	<MRV		Locker near a laboratory door	<MRV
		<MRV			<MRV
		<MRV			<MRV

MRV: minimum reporting value

5.2.2.3 Site S8

Table 24 shows counts of particles collected over a production day on microscopy grids directly placed in grid holders. Holders 1 and 2 (placed about 1 m apart) were positioned right on an automatic varnishing machine at the worker's breathing zone height (1 m 60 cm). Holder 3 was placed in the adjacent room, where the varnished boards are packaged. Particle quantities deposited on the grids were similar in the case of holders 1 and 2, but fewer particles were deposited on the grid in holder 3 (Table 24). The particles on the grid in holder 3 nonetheless confirmed that this work area is contaminated by NPs from the adjacent room. Figure 32 shows images of these deposited particles. Note the agglomerated spherical particles of SiO_2 and the rod-shaped particles of TiO_2 measuring 10 nm x 100 nm and identified as a form of rutile.

Table 24 – TEM/EDS counts of TiO_2 and SiO_2 particles deposited by diffusion and collected using grid holders at site S8

	TiO_2		SiO_2	
	Particle count	%	Particle count	%
Holder 1 (varnishing area)	57	83	12	17
Holder 2 (varnishing area)	61	86	10	14
Holder 3 (packaging area)	6	35	11	65

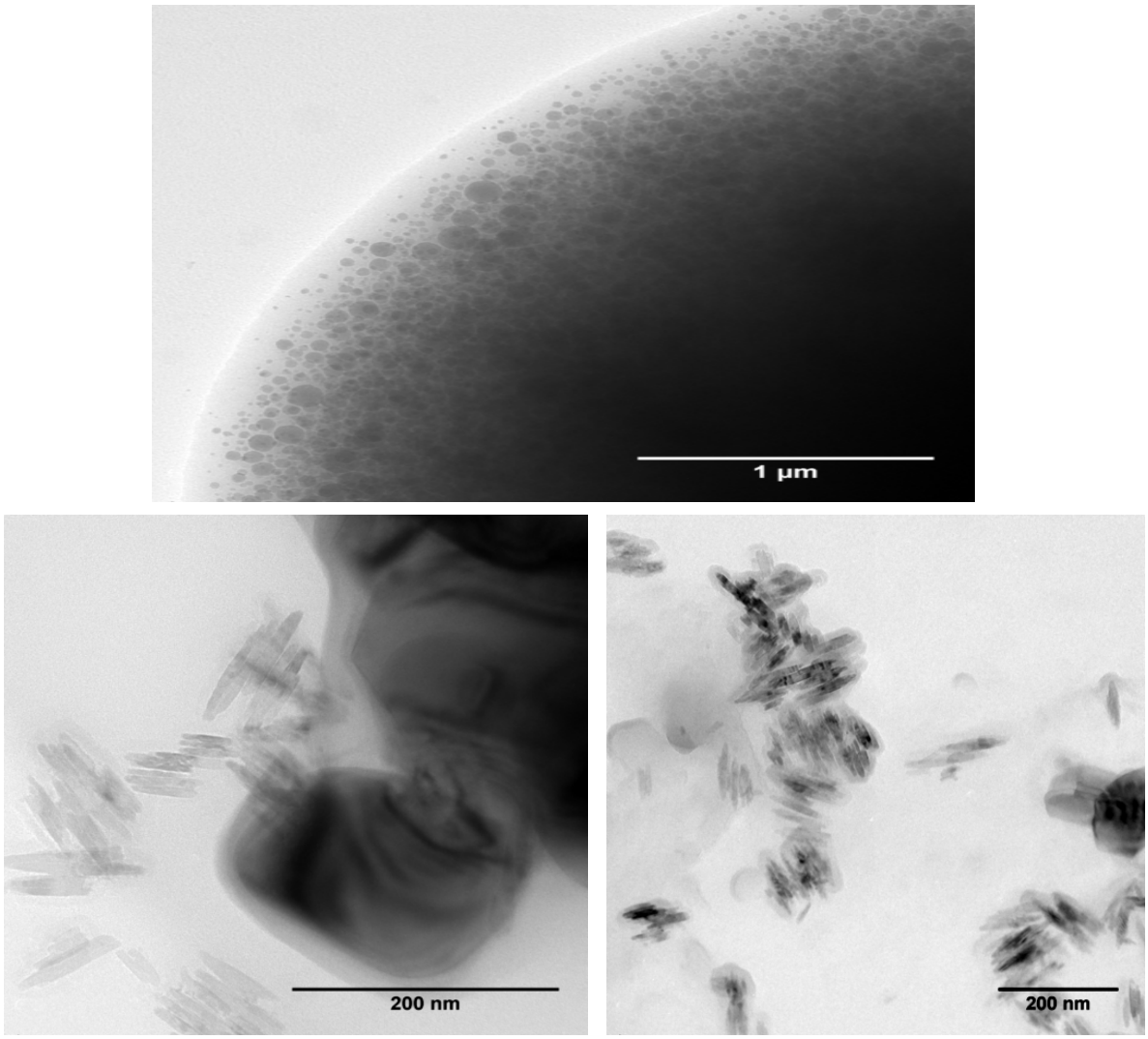

Figure 32 – TEM images of particles collected on grids at site S8.

6. DISCUSSION

This research project has two complementary parts: a laboratory investigation and a fieldwork component. The first part of the project, Part A, involved generating TiO_2 nanoparticles under controlled laboratory conditions and then studying different sampling and analysis techniques. The second part, Part B, comprised a series of nine field studies adapted to different workplaces (sites S1 to S9) and designed to test a variety of sampling devices and analytical procedures and to measure ENM exposure levels among Québec workers.

6.1 Assessment and development of characterization methods and techniques

6.1.1 Part A – laboratory investigation

Part A yielded original results showing there is no linear relationship between NP morphological parameters determined via electron microscopy image processing and duration of simulated exposure. Microscopy grid saturation was noted, limiting the possibility of using image analysis to quantify exposure. Sampling time, it seems, is a factor that must be considered when using a grid to collect airborne particles in the workplace. Overloading of microscopy grids can lead to overestimation of average particle agglomerate size and underestimation of particle concentrations. Our results thus suggest that sampling time should be limited when high contaminant concentrations are suspected to minimize uncertainty about particle overloading of the grids. This same concern regarding sampling time has been reported in the literature (Asbach, 2016). However, it is important to note that for the laboratory investigations, relatively high contaminant concentrations were used compared to those generally found in the workplace (Debia et al., 2016).

6.1.2 Part B – fieldwork

A satisfactory assessment of potential occupational exposure was obtained using a multimetric approach (combining a series of real-time and integrated measurements) at nine worksites.

At most of the workplaces studied, DRIs designed for ultrafine particle detection (EEPS and P-Trak CPC) did not prove effective in identifying particulate emissions, except at sites S3 and S5. On the other hand, the DustTrak DRX (laser photometer) worked well at all study sites. The large ENM agglomerates identified by microscopy corroborate these results, given that sites S3 and S5 are those where the principal modes of generation seemed the weakest. The presence of airborne ENM agglomerates in these environments is already well documented (Debia et al., 2016).

However, there are no recognized methods of interpreting DRI results that consider background concentrations. A process-to-background ratio, as described by Cena and Peters (2011) and systematically calculated for sites S1 to S9, offers an interesting perspective, giving results that are easy to interpret in case of strong generation or regular generation over several minutes—when sanding or spraying varnish, for example (sites S6, S8 and S9). However, relying on ratios

can be misleading in the case of tasks of short duration (such as sawing) or in environments with high background concentrations (e.g., hot processes or presence of ultrafine particles) (site S6). In such cases, examination of graphical profiles can make it possible to confirm particle generation potential.

While sampling with microscopy grids glued to filters made it possible to systematically confirm presence of the NPs of interest in the workplaces, the MPS seems an especially promising approach to improve performances with metal oxides as well as CNTs. This new and more effective sampling device gives a more precise fibre count (see Section 5.2.1.3.2.1) without any sample handling. A concentration of 0.108 SWCNTs/cm³ was thus measured in a worker's breathing zone at site S1.

Three methods of sampling CNTs and CNFs were tested simultaneously to determine a worker's personal exposure at site S1: a BGI GK2.69 cyclone was used to collect a respirable fraction; a PPI impactor was used to collect a respirable fraction; and another PPI impactor was used to collect a thoracic fraction. EC analyses were then performed using the NIOSH 5040 method. Though EC was not detected in the aerosols when sampling with the GK2.69 cyclone, it was detected in the samples collected with the two PPIs, and in both cases concentrations were above the exposure level recommended by NIOSH (1 µg/m^3) (NIOSH, 2013). Note that we did not weight the results to get an 8-hour time-weighted average as our goal was to characterize the work activity rather than worker exposure. In addition, it has been demonstrated that EC concentrations measured in the respirable fraction reflect only half those in the thoracic fraction, whereas particles in both fractions can enter and settle in a worker's airways. Measurement of the respirable fraction alone may thus give an underestimation of exposure.

Analyses performed for this project during production of SWCNTs at site S1 highlighted an important limitation of the EC measurement method stemming from interference with carbon black particles. Kuhlbusch et al. (2004) report that concentrations of EC accounted for 46% to 92% of the PM_{10} mass concentrations of particles emitted during packaging of various kinds of carbon black. Chai et al. (2012) describe a method for validating EC measurements obtained with the NIOSH 5040 method using filters first loaded with carbon black. The microscopy analyses demonstrated the presence of highly agglomerated spherical carbon particles identified as carbon black, which is used as a carbon source in SWCNT production. The particle counts thus showed that only about 5% of the particles on the microscopy grids are or contain SWCNTs. Additional analyses using Raman spectroscopy also indicated that only four of 16 spectra had profiles showing presence of SWCNTs and that the quantity of SWCNTs in the analyses was less than 6%. The other spectra corresponded to carbon black particles. In other words, there is uncertainty as to the efficacy of the NIOSH 5040 method for assessing exposure to CNTs and CNFs, especially when dealing with producers of these NPs and users of raw, unpurified products where presence of carbon black is highly likely.

In this project, we also successfully tested the ICP-MS analysis technique for assessing metal oxides using personal samples as well as fixed-station samples. As described in Section 2, a number of researchers also report collection of samples on filters for subsequent ICP-MS analysis to quantify exposure to metal oxides such as aluminum oxides, TiO_2 and iron oxides

(Berges et al., 2007; Lee et al., 2012; Lee et al., 2011; Methner et al., 2010a; Methner et al., 2010b; Shepard and Brenner, 2014b)

Lastly, surface analyses for this project, with active (sampling pump) or passive (grid holder) sampling, made it possible to assess ENM dispersion through the workplace. The analyses showed dispersion at site S8, but containment of the production area at site S1. At site S4, contamination of change rooms with titanium NPs and carbon fibres was established, but the efficacy of cleaning was also confirmed at this site by a pre- and post-cleaning comparison.

6.2 Development of an improved assessment strategy

Based on the assessments performed for this project, we propose an innovative strategy for more accurate assessment of ENM exposure that combines techniques and methods requiring a minimum of preanalytic handling. A two-phase strategy is recommended for systematic assessment of workplaces where ENMs are produced and used.

6.2.1 Phase 1: Preliminary assessment

As a first step, DRIs should be used to identify the work tasks that generate ENMs. It is recommended that at least a CPC and a laser photometer be used to assess ENM generation. These instruments are portable and relatively simple to use, and there are no analysis costs (other than the costs of purchase, maintenance and annual calibration). An OPC can however be used instead of a laser photometer, and an ELPI can replace both instruments as it covers the range of a CPC and an OPC or laser photometer.

The DRI measurements must be completed by air and surface sampling for subsequent microscopy analysis (MPS + SEM/TEM-EDS) to confirm ENM nature, shape and agglomeration. Analysis of about 20 particles is sufficient to confirm the presence of ENMs and perform a basic characterization of the particles collected.

6.2.2 Phase 2: In-depth assessment

When occupational exposure is confirmed, more elaborate quantification may be desirable. In this second step of exposure quantification, ENMs identified are specifically targeted. Metal oxides can be quantified using ICP-MS. CNTs and CNFs can be quantified by EC analyses, according to NIOSH recommendations, with samples collected using a variety of techniques. It is recommended that these measurements be coupled with an MPS/Raman quantitative analysis to determine the quantity of CNTs in the samples, especially when presence of carbon black is suspected.

Depending on the situation, complementary surface analyses can also be performed at this stage to assess workplace contamination and the efficacy of control measures (containment, cleaning of premises and local exhaust ventilation).

6.3 Findings with respect to control measures

For each field study performed as part of this project, a customized report was submitted to the participating company and, as needed, a presentation was given in the workplace. The reports described the methods and the results of the real-time measurements and quantitative microscopy analyses. An assessment of exposure levels and control measures was included as well as some recommendations. This section briefly summarizes our main findings: Use of glove boxes, laboratory hoods and/or local exhaust ventilation systems was noted in a number of workplaces (at sites S1, S3, S4, S6 and S8). The glove boxes were deemed extremely effective in containing ENMs at the source. Our field studies showed most laboratory hoods were highly or relatively effective. However, it was demonstrated that particles can escape from the hoods during certain activities. Harvesting nanopowders directly into a leak-tight bag at the reactor outlet is another effective at-source control measure (S1). Containment of specific areas of process steps particularly likely to generate nanomaterials as well as complete process containment in a dedicated room with its own ventilation system are other control measures that proved effective (S1, S2 and S4). At two sites with dedicated areas, there were adjacent changing rooms (one or two) to prevent cross contamination (S1 and S4). Lastly, at most of the workplaces, individual respiratory protection and personal protective equipment for skin protection were used, including half masks, full masks, hoods with filtering systems, motorized filtering systems or air supply systems, Tyvek®-type suits and lab coats. Note that only lab coats of non-woven materials should be used (Ostiguy, 2014). Armguards and gloves were also noted, providing skin protection and preventing contamination of other areas in the workplace.

7. GENERAL CONCLUSIONS

This research on methods of sampling and characterizing ENMs was carried out by a multi-disciplinary team with members from the Université de Montréal, Polytechnique Montréal and the IRSST. The goal was to promote the safe development of nanotechnologies in Québec, a rapidly growing sector where the number of workers possibly exposed to ENMs is increasing incessantly.

As there are still many unanswered questions about the health effects of chronic exposure to ENMs, a preventive approach is recommended. Exposure assessment is a crucial step in this approach. Based on a review of recent scientific literature on ENM exposure, an assortment of techniques and measuring instruments were tested on a wide variety of ENMs (nanotubes, TiO_2, SiO_2, nanofibres, etc.). There are, however, many other instruments available that were not tested in this project. The reader is referred to the NanoIndEx report for additional information on sampling and measuring instruments (Asbach, 2016). In the meantime, applications that use nanomaterials are increasing very rapidly, and, as mentioned, the growth in the number of workers exposed parallels this trend. It is thus critical to proceed as outlined herein in order to identify and better understand the industries and workplaces where workers are most exposed and to document exposure intensity.

One of the important features of this study is that producers as well as users of ENMs were investigated: in total, nine Québec workplaces were visited. A second important feature was the combination of airborne and surface measurements. As a result, it was possible to begin the work of quantifying ENMs using microscopy. The first results are encouraging, but the investigations must be continued, especially with respect to sampling time and counting methods (technique and surface area).

Lastly, the study made it possible to suggest strategies for assessing occupational exposure to different ENMs. Cost and feasibility in the workplace were not considered but should be examined in the future: e.g., drafting of specifications for design of an inexpensive, portable, versatile and user-friendly ENM detector. It is important to mention, as well, that this study looked at methods of sampling and characterizing ENMs but was not meant to come up with an integrated approach to the management of risks associated with using ENMs. For questions of risk management, the reader is referred to *Best Practices Guidance for Nanomaterial Risk Management in the Workplace* (Ostiguy et al., 2014).

BIBLIOGRAPHY

AFSSET, 2008. Évaluation des risques liés aux nanomatériaux pour la population générale et pour l'environnement. Agence française de sécurité sanitaire de l'environnement et du travail. Rapport d'expertise collectif, Comité d'experts spécialisés “Agents physiques, nouvelles technologies et grands aménagements,” Groupe de Travail “Nanomatériaux - exposition du consommateur et de l'environnement.” Saisine No. 2008/005, 207 p.

Asbach, C., et al., 2016. Assessment of personal exposure to airborne nanomaterials: A guidance document. NanoIndEx.
http://www.nanoindex.eu/wp-content/uploads/2016/06/Nano_Brosch%C3%BCre.pdf

ASTM, 2008. D6966 − 08, Standard practice for collection of settled dust samples using wipe sampling methods for subsequent determination of metals.
https://www.astm.org/Standards/D6966.htm\

ASTM, 2014. D5755 Standard test method for microvacuum sampling and indirect analysis of dust by transmission electron microscopy for asbestos structure number surface loading. http://www.astm.org/Standards/D5755.htm.

Baron, A.A., et al., 2002. Evaluation of aerosol release during the handling of unrefined single-walled carbon nanotube material. National Institute for Occupational Safety and Health, 22 p.

Bello, D., et al., 2008. Particle exposure levels during CVD growth and subsequent handling of vertically-aligned carbon nanotube films. Carbon 46:974-977.

Bello, D., et al., 2009. Exposure to nanoscale particles and fibres during machining of hybrid advanced composites containing carbon nanotubes. J Nanopart Res 11:231-249.

Bello, D., et al., 2010. Characterization of exposures to nanoscale particles and fibres during solid core drilling of hybrid carbon nanotube advanced composites. Int J Occup Environ Health 16:434-450.

Berges, M., et al., 2007. Workplace exposure characterization at TiO2 nanoparticle production site. Proceedings of the 3rd International Symposium on Nanotechnology, Occupational and Environmental Health, Taipei, Taiwan, 183-184.

Birch, M.E., et al., 2011. Exposure and emissions monitoring during carbon nanofibre production--Part I: elemental carbon and iron-soot aerosols. Ann Occup Hyg 55:1016-1036.

Brouwer, D., et al., 2013. Workplace air measurements and likelihood of exposure to manufactured nano-objects, agglomerates, and aggregates. J Nanopart Res 15:1-14.

Cena, L., et al., 2015. A field study on the respiratory deposition of the nano-sized fraction of mild and stainless steel welding fume metals. J Occup Environ Hyg, 12(10):721-728.

Cena, L., et al., 2014. A novel method for assessing respiratory deposition of welding fume nanoparticles. J Occup Environ Hyg 11:771-780.

Cena, L., et al., 2011. A personal nanoparticle respiratory deposition (NRD) sampler. Environ Sci Technol 45:6483-6490.

Cena, L. and Peters, T.M., 2011. Characterization and control of airborne particles emitted during production of epoxy/carbon nanotube nanocomposites. J Occup Environ Hyg 8:86-92.

Chai, M., et al., 2012. Organic and elemental carbon filter sets: preparation method and interlaboratory results. Ann Occup Hyg 56:959-67.

Dahm, M.M., et al., 2013. Occupational exposure assessment in carbon nanotube and nanofibre primary and secondary manufacturers: mobile direct-reading sampling. Ann Occup Hyg 57:328-344.

Dahm, M.M., et al., 2012. Occupational exposure assessment in carbon nanotube and nanofibre primary and secondary manufacturers. Ann Occup Hyg 56:542-556.

Debia, M., et al., 2012a. Caractérisation et contrôle de l'exposition professionnelle aux nanoparticles et particles ultrafines. Institut de recherche Robert-Sauvé en santé et en sécurité du travail (IRSST). Report R-746, 66 pages.
https://www.irsst.qc.ca/media/documents/PubIRSST/R-746.pdf.

Debia, M., et al., 2012b. Ultrafine particle (UFP) exposures in an aluminium smelter: Soderberg vs. prebake potrooms. Environ Pollut 1:2-12.

Debia, M. et al., 2016 . A systematic review of reported exposure to engineered nanomaterials. Ann Occup Hyg 2016:1-20.

Endo, C.A., et al., 2014. Portrait de la nanotechnologie au Québec dans les milieux industriels et de la recherche universitaire et publique. Institut de recherche Robert-Sauvé en santé et en sécurité du travail (IRSST). Report R-854, 104 pages
http://www.irsst.qc.ca/media/documents/PubIRSST/R-854.pdf.

Evans, D.E., et al., 2010. Aerosol monitoring during carbon nanofibre production: mobile direct-reading sampling. Ann Occup Hyg 54:514-531.

Fleury, D., et al., 2013. Identification of the main exposure scenarios in the production of CNT-polymer nanocomposites by melt-moulding process. J Clean Prod 53:22-36.

Fujitani, Y. and Kobayashi, T., 2008. Measurement of aerosols in engineered nanomaterials factories for risk assessment. Nano 03:245-249.

Han, J.H., et al., 2008. Monitoring multiwalled carbon nanotube exposure in carbon nanotube research facility. Inhal Toxicol 20:741-749.

Heitbrink, W.A., et al., 2013. Case study: particle emissions from the processes of machining nanocomposites. EPHB Report No. EPHB 356-19a. 63 pages.

Huang, G., et al., 2012. Evaluation of airborne particle emissions from commercial products containing carbon nanotubes. J Nanopart Res 14:1-3.

Johnson, D.R., et al., 2010. Potential for occupational exposure to engineered carbon-based nanomaterials in environmental laboratory studies. Environ Health Persp 118:49-54.

Koivisto, A., et al., 2012. Industrial worker exposure to airborne particles during the packing of pigment and nanoscale titanium dioxide. Inhal Toxicol 24:839-849.

Ku, B.K., et al., 2007. Observation and measurement of anomalous responses in a differential mobility analyzer caused by ultrafine fibrous carbon aerosols. J Electrostat 65:542-548.

Kuhlbusch, T., et al., 2011. Nanoparticle exposure at nanotechnology workplaces: a review. Part Fibre Toxicol 8:1-22.

Kuhlbusch, T., et al., 2004. Number size distribution, mass concentration, and particle composition of PM1, PM2.5, and PM10 in bag filling areas of carbon black production. J Occup Environ Hyg 1:660-671.

Lee, J.H., et al., 2012. Continuous 3-day exposure assessment of workplace manufacturing silver nanoparticles. J Nanopart Res 14:1-10.

Lee, J.H., et al., 2011. Exposure assessment of workplaces manufacturing nanosized TiO2 and silver. Inhal Toxicol 23:226-236.

Lee, S.-B., et al., 2010. In-situ characterization of metal nanopowders manufactured by the wire electrical explosion process. Aerosol Sci Technol 44:1131-1139.

Leskinen, J., et al., 2012. Comparison of nanoparticle measurement instruments for occupational health applications. J Nanopart Res 14:1-16.

Lo, L.M., et al., 2013. Assessment of nanoparticle emissions from a chemical laboratory using carbon nanotubes. EPHB Report No. 356-18a. 36 pages.

Maynard, A., et al., 2007. Measuring particle size-dependent physicochemical structure in airborne single walled carbon nanotube agglomerates. J Nanopart Res 9, 85-92.

Maynard, A.D., et al., 2004. Exposure to carbon nanotube material: aerosol release during the handling of unrefined single-walled carbon nanotube material. J Toxicol Environ Health. Part A 67, 87-107.

Methner, M., et al., 2012a. Field application of the nanoparticle emission assessment technique (NEAT): task-based air monitoring during the processing of engineered nanomaterials (ENM) at four facilities. J Occup Environ Hyg 9:543-555.

Methner, M., et al., 2012b. Evaluation of the potential airborne release of carbon nanofibres during the preparation, grinding, and cutting of epoxy-based nanocomposite material. J Occup Environ Hyg 9:308-318.

Methner, M., et al., 2010a. Nanoparticle emission assessment technique (NEAT) for the identification and measurement of potential inhalation exposure to engineered nanomaterials—Part B: Results from 12 field studies. J Occup Environ Hyg 7:163-176.

Methner, M., et al., 2010b. Nanoparticle emission assessment technique (NEAT) for the identification and measurement of potential inhalation exposure to engineered nanomaterials—Part A. J Occup Environ Hyg 7:127-132.

Monteiro-Riviere, N.A. and Riviere, J.E., 2009. Interaction of nanomaterials with skin: aspects of absorption and biodistribution. Nanotoxicology 3:188-193.

Motellier, S., et al., 2011. Direct quantification of airborne nanoparticles composition by TXRF after collection on filters. J Phys Conf Ser 304(1):012009.

Nilsson, P., et al., 2013. Nano-objects emitted during maintenance of common particle generators: direct chemical characterization with aerosol mass spectrometry and implications for risk assessments. J Nanopart Res 15:1-16.

NIOSH, 2003. NIOSH Method 5040: Issue 3. Diesel particulate matter (as elemental carbon). http://www.cdc.gov/niosh/docs/2003-154/pdfs/5040.pdf.

NIOSH, 2009. Approaches to safe nanotechnology: managing the health and safety concerns associated with engineered nanomaterials. NIOSH Publication 2009-125, 104 pages, http://www.cdc.gov/niosh/docs/2009-125/pdfs/2009-125.pdf.

NIOSH, 2011. Nanotechnology, 10 critical topic areas. http://www.cdc.gov/niosh/topics/nanotech/critical.html.

NIOSH, 2013. Occupational exposure to carbon nanotubes and nanofibres. Current Intelligence Bulletin 65. https://www.cdc.gov/niosh/docs/2013-145/pdfs/2013-145.pdf.

Noël, A., et al., 2013. Generating nano-aerosols from TiO_2 (5 nm) nanoparticles showing different agglomeration states: application to toxicological studies. J Occup Environ Hyg 10:86-96.

Ogura, I., et al., 2011. Onsite aerosol measurements for various engineered nanomaterials at industrial manufacturing plants. J Phys Conf Ser 304 (1):012004.

Ono-Ogasawara M. and Myojo, T., 2011. A proposal of method for evaluating airborne MWCNT concentration. Ind Health 49:726-734.

Ono-Ogasawara, M., et al., 2013. Approach to the exposure assessment of MWCNT by considering size distribution and oxidation temperature of elemental carbon. J Phys Conf Ser 429(1):012004.

Ostiguy, C., et al., 2010. Les nanoparticles de synthèse : connaissances actuelles sur les risques et les mesures de prévention en SST. 2nd edition. Institut de recherche Robert-Sauvé en santé et en sécurité du travail (IRSST). Report-646, 159 pages. https://www.irsst.qc.ca/media/documents/PubIRSST/R-646.pdf.

Ostiguy, C., et al., 2008. Les effets sur la santé reliés aux nanoparticles. 2nd edition. Institut de recherche Robert-Sauvé en santé et en sécurité du travail (IRSST). Report R-558, 120 pages. https://www.irsst.qc.ca/media/documents/PubIRSST/R-558.pdf.

Ostiguy, C., et al., 2014. Best practices guidance for nanomaterial risk management in the workplace. 2nd edition. Institut de recherche Robert-Sauvé en santé et en sécurité du travail (IRSST). Report R-899, 113 pages. http://www.irsst.qc.ca/media/documents/PubIRSST/R-899.pdf.

Peters, T.M., et al., 2009. Airborne monitoring to distinguish engineered nanomaterials from incidental particles for environmental health and safety. J Occup Environ Hyg 6:73-81.

Rasmussen, P.E., et al., 2013. Metal impurities provide useful tracers for identifying exposures to airborne single-wall carbon nanotubes released from work-related processes. J Phys Conf Ser 429(1):012007.

R'Mili, B., et al., 2011. Analysis of particle release using LIBS (laser-induced breakdown spectroscopy) and TEM (transmission electron microscopy) samplers when handling CNT (carbon nanotube) powders. J Nanopart Res 13:563-577.

R'Mili, B., et al., 2013. Particle sampling by microscopy grid filtration. Aerosol Sci Technol 47:767-775.

Raynor, P.C., et al., 2012. Assessing potential nanoparticle release during nanocomposite shredding using direct-reading instruments. J Occup Environ Hyg 9:1-13.

Reed, R.B., et al., 2013. Detection of single walled carbon nanotubes by monitoring embedded metals. Environ Sci Process Impact 15:204-213.

Riviere, J.E., et al., 2012. Acute vascular effects of nanoparticle infusion in isolated perfused skin. Nanomed Nanotech Biol Med 8:428-431.

Saathoff, J.G., et al., 2011. In vitro toxicity assessment of three hydroxylated fullerenes in human skin cells. Toxicol in Vitro 25:2105-2112.

Safe Work Australia, 2010. Developing workplace detection and measurement techniques for carbon nanotubes. http://www.safeworkaustralia.gov.au/sites/swa/about/publications/pages/rp201006developingworkplacedetectionandmeasurement.

Sahu, M. and Biswas, P., 2010. Size distributions of aerosols in an indoor environment with engineered nanoparticle synthesis reactors operating under different scenarios. J Nanopart Res 12:1055-1064.

Schaeublin, N.M., et al., 2012. Does shape matter? Bioeffects of gold nanomaterials in a human skin cell model. Langmuir 28:3248-3258.

Schlagenhauf, L., et al., 2012. Release of carbon nanotubes from an epoxy-based nanocomposite during an abrasion process. Environ Sci Technol 46:7366-7372.

Shepard, M. and Brenner, S., 2014a. Cutaneous exposure scenarios for engineered nanoparticles used in semiconductor fabrication: a preliminary investigation of workplace surface contamination. Int J Occup Environ Health 20:247-257.

Shepard, M.N. and Brenner, S., 2014b. An occupational exposure assessment for engineered nanoparticles used in semiconductor fabrication. Ann Occup Hyg 58:251-265.

Shvedova, A.A., et al., 2012. Mechanisms of carbon nanotube-induced toxicity: focus on oxidative stress. Toxicol Appl Pharmacol 261:121-133.

Stone, V., et al., 2010. Engineered nanoparticles: review of health and environmental safety (ENRHES). Project Final Report. European Commission.

Tsai, C.S-J., 2013. Potential inhalation exposure and containment efficiency when using hoods for handling nanoparticles. J Nanopart Res 15:1-12.

Tsai, C.S-J., et al., 2012. Exposure assessment and engineering control strategies for airborne nanoparticles: an application to emissions from nanocomposite compounding processes. J Nanopart Res 14:1-14.

Tsai, C,S-J., et al., 2009a. Characterization and evaluation of nanoparticle release during the synthesis of single-walled and multiwalled carbon nanotubes by chemical vapor deposition. Environ Sci Technol 43:6017-6023.

Tsai, C.S-J., et al., 2009b. Airborne nanoparticle exposures associated with the manual handling of nanoalumina and nanosilver in fume hoods. J Nanopart Res 11:147-161.

Van der Merwe, D., et al., 2009. Nanocrystalline titanium dioxide and magnesium oxide in vitro dermal absorption in human skin. Cutan Ocul Toxicol 28:78-82.

Van Landuyt, K.L., et al., 2014. Nanoparticle release from dental composites. Acta Biomater 10:365-374.

Vance, M.E., et al., 2015. Nanotechnology in the real world: redeveloping the nanomaterial consumer products inventory. Beilstein J Nanotechnol 6:1769-1780.

Vorbau, M., et al., 2009. Method for the characterization of the abrasion induced nanoparticle release into air from surface coatings. J Aerosol Sci 40:209-217.

Witschger, O., et al., 2012. Préconisations en matière de caractérisation des potentiels d'émission et d'exposition professionnelle aux aérosols lors d'opérations mettant en oeuvre des nanomatériaux. Hygiène et Sécurité du travail 226:41-55.

Woskie, S.R., et al., 2010. Understanding workplace processes and factors that influence exposures to engineered nanomaterials. Int J Occup Environ Health 16:365-377.